

New biostratigraphy and microfacies analysis of Eocene Jahrum Formation (Shahrekord region, High Zagros, West Iran). A carbonate platform within the Neo-Tethys oceanic realm

Seyed Ahmad Babazadeh^{1,*} and Dominique Cluzel²

¹ Department of Sciences, Payame Noor University, Po. Box 19395-3697, Tehran, Iran

² Institut de Sciences Exactes et Appliquées, Université de la Nouvelle-Calédonie, BP R4, 98851 Noumea Cedex, New Caledonia

Received: 26 March 2021 / Accepted: 14 October 2022 / Publishing online: 26 January 2023

Abstract – The Eocene Jahrum Formation in High Zagros was studied in Kuh-e- Soukhteh and North Gahrou sections (southwest of Shahrekord region, Chahar-mahal Bakhtiari Province). This formation, composed of limestone, marl, and dolomitic limestone (dolostone), accumulated on a marine platform within the Neo-Tethys ocean realm. It yields a rich foraminiferal fauna, in which three larger benthic foraminiferal assemblage zones were identified. Two assemblage zones in the North Gahrou section were correlated to the Ypresian and Bartonian, and one assemblage zone is represented in the Kuh-e- Soukhteh section and assigned to the Bartonian. In addition, three other groups of benthic foraminiferal associations have been identified based on test wall type (porcellaneous, agglutinate, hyaline) and paleogeographical significance. A discontinuity marked by a hiatus from Cuisian to Lutetian in the North Gahrou section was most probably due to a concealed fault. According to microscopic textures and distribution of benthic foraminifera and other components (peloids, intraclasts, etc.), a gentle depth gradient from the inner ramp to the proximal outer ramp may be reconstructed.

Keywords: stratigraphy / microfacies / larger foraminifera / Jahrum Formation / High Zagros / West Iran

Résumé – **Nouvelle biostratigraphie et analyse des microfaciès de la Formation éocène de Jahrum (région de Shahrekord, Haut Zagros, Iran occidental). Une plateforme carbonatée au sein de la néo-téthys.** La formation éocène de Jahrum dans le Haut Zagros a été étudiée le long de deux coupes, Kuh-e-Soukhteh et Gahrou-nord (sud-ouest de la Région de Shahrekord, Province de Chahar-mahal Bakhtiari). Cette formation composée de calcaires, marnes et calcaires dolomitiques, s'est déposée en contexte de plateforme au sein du domaine océanique néo-téthysien. La riche faune de foraminifères a permis d'identifier trois biozones de grands foraminifères benthiques. Deux biozones de la coupe de Gahrou-nord sont corrélées respectivement à l'Yprésien et au Bartonien tandis qu'une seule zone assignée au Bartonien a été définie dans la coupe de Kuh-e- Soukhteh. De plus, trois autres groupes d'associations de foraminifères benthiques ont été identifiés selon le type de test (porcellané, agglutiné, hyalin) et leur signification paléogéographique. L'absence du Cuisien et du Lutétien dans la coupe de Gahrou-nord est probablement due à une faille cachée. La distribution des microfaciès, des foraminifères benthiques et autres composants (peletoïdes, intraclastes) permet de reconstituer un gradient modéré de profondeur évoluant depuis la rampe interne jusqu'à la rampe externe proximale.

Mots clés : stratigraphie / microfaciès / grands foraminifères / formation de Jahrum / Haut Zagros / Iran occidental

*Corresponding author: seyedbabazadeh@yahoo.com; sababazadeh@pnu.ac.ir

1 Introduction

The geological history of Iran recorded several tectonic events related to the Alpine-Himalayan orogeny, which resulted from the collision of the Arabian Platform and several derived microcontinents with Eurasia. Several tectonic phases have contributed to the separation of sedimentary-tectonic basins within the Iran platform, which may be distinguished based on sedimentary facies and benthic foraminiferal communities. After the Paleo-Tethys closure in northern Iran (Alborz Margin) during the Middle Triassic, rifting and oceanization (Neo-Tethys Realm) occurred again in southwestern and eastern Iran since the Lower Cretaceous, the traces of which are now distributed along the main Zagros Thrust. As a consequence, the ancient Gondwana Margin was fragmented into some microcontinents separated by marginal basins. Afterward, the different microcontinents shifted gradually northward and collided with Eurasia during the Late Cretaceous to Upper Eocene period. The closure of marginal basins by subduction formed ophiolitic belts, *i.e.*, assemblages of ultrabasic and basaltic rocks, pelagic sediments (radiolarian cherts and pelagic limestones), and subduction-related (high-pressure low-temperature) metamorphic rocks (Berberian and King, 1981; Babazadeh, 2003; Babazadeh and De Wever, 2004a, 2004b). The continental collision of the Arabian and Eurasian Plates resulted in the formation of the Zagros Mountains (Takin, 1972; Agard *et al.*, 2005). They are located in the middle part of the Alpine-Himalayan Orogenic Belt as a narrow northwest-southeast trending domain, which extends from the Taurus (northeast of Turkey) to the Hormuz Strait (southwest Iran) (Alavi, 2004) (Fig. 1). Owing to the occurrence of several oil formations, detailed research was carried out on the Neo-Tethysian Zagros sedimentary basin. Special attention was paid to its Cenozoic components, which include the Jahrum Formation, a shallow marine carbonate platform unit of special interest because it is one of the important reservoirs in the Zagros and Persian Gulf oil province. However, despite many lithological and paleontological investigations conducted in different parts of Zagros (James and Wynd, 1965; Kalantari, 1976, 1978, 1980, 1986, 1992; Stocklin and Setudehnia, 1991; Rahaghi, 1976, 1978, 1980, 1983; Khatibi Mehr and Moalemi, 2009; Babazadeh *et al.*, 2015; Babazadeh and Pazooki Ranginlou, 2015) a precise paleo-environmental framework for Jahrum Formation remains to be established. The purpose of this study is: 1) to provide more data about microfacies and reconstruct the evolution of the depositional environment in a well-constrained stratigraphic framework during the Eocene; 2) to introduce three foraminiferal biozones for correlation with Eocene benthic foraminifera associations of east Iran and neighboring countries (Pakistan and Turkey) and standard biozonation scales of west Tethys.

2 Geologic setting

Because of the regional NW-SE structural trend, the Shahrekord region is subdivided into northeast (Z1), central (Z2), and southwest (Z3) fault-bounded zones (Fig. 2A). The Central Zone (Z2) which is the object of the study in this article, consists of the Gurpi, Jahrum, Pabdeh, and Asmari

formations composed of Late Cretaceous to Paleogene red clastic rocks, gray to cream limestone, and marl (Zahedi and Rahmati Ilkhechi, 2006).

The Jahrum Formation at the type section consists of gray to yellow dolomitic limestone and dolomite with a sugary texture. The basal contact of this formation is conformable with Maastrichtian-Paleocene Sachun Formation but its top is covered by a regional disconformity with Oligo-Miocene Asmari Formation (James and Wynd, 1965).

Two stratigraphic sections (Kuh-e-Soukhteh and North Gahrou sections) were selected and measured in the southwest of the Shahrekord region from the Gahrou area (Chahar-mahal Bakhtiari province). In the studied sections, the Jahrum Formation consists of alternating thick layers of massive limestone interbedded with softer fine-grained limestone, dolomitic limestone (dolostone), and marl. The basal contact of the Jahrum Formation with the underlying Pabdeh Formation is faulted in both sections, while its upper boundary is an unconformity contact with the overlying Asmari Formation, or is covered by alluvium. The stratigraphic sections are located in a quadrant limited by N 32°00' to N 32°06' Long. and E 50°55' to E 51°00' Lat. (Fig. 2B).

3 Materials and methods

The two sections were measured over a thickness of 157 m and 215 m respectively and approximately 165 samples were collected in the field. All specimens were stored and studied at the geological laboratory of Tehran Payame Noor University, Iran. Micro-texture analysis and micro-paleontological determinations were performed under the plane light microscope. Biotic and abiotic components such as foraminifers, bioclasts, peloids, lumps, and intraclasts were determined after Rahaghi (1980), Loeblich and Tappan (1987), Serra-Kiel *et al.* (1998), Hottinger (2007), Sirel (2003, 2009), Dunham (1962), Embry and Klovan (1971), Buxton and Pedley (1989) and Flugel (2004).

4 Regional lithostratigraphy

Three structural zones are documented by the regional NW-SE trend in the Shahrekord region of Chahar-mahal Bakhtiari Province (Zahedi and Rahmati Ilkhechi, 2006). The Northeast Zone (Z1) in the northeast of Zayandehrud consists of metamorphic rocks unconformably overlain by Permian basal conglomerate with metamorphic rock clasts embedded in siliceous cement. In turn, the conglomerate is overlain by Triassic, Jurassic, and Cretaceous marine platform deposits.

The Central Zone (Z2) is a part of the High Zagros and is located between the Saman-Fereidoon Shahr Thrust (F1) and the Bazoft Thrust (F3). Based on the main Zagros Thrust Fault, this zone is divided into two smaller sub-zones: Z2a and Z2b. These two sub-zones consist of the Gurpi, Jahrum, Pabdeh, and Asmari formations composed of Late Cretaceous to Paleogene red clastic rocks, gray to cream limestone, and marl.

The Southwest Zone (Z3) is located southwest of the Karun River and Karun Mountains. It consists of Mesozoic and Cenozoic black shale, siltstone, and thin limestone and forms a large part of the Zagros sedimentary basin. This zone is separated from Z2 by the SW-verging Bazoft Thrust (F3). The

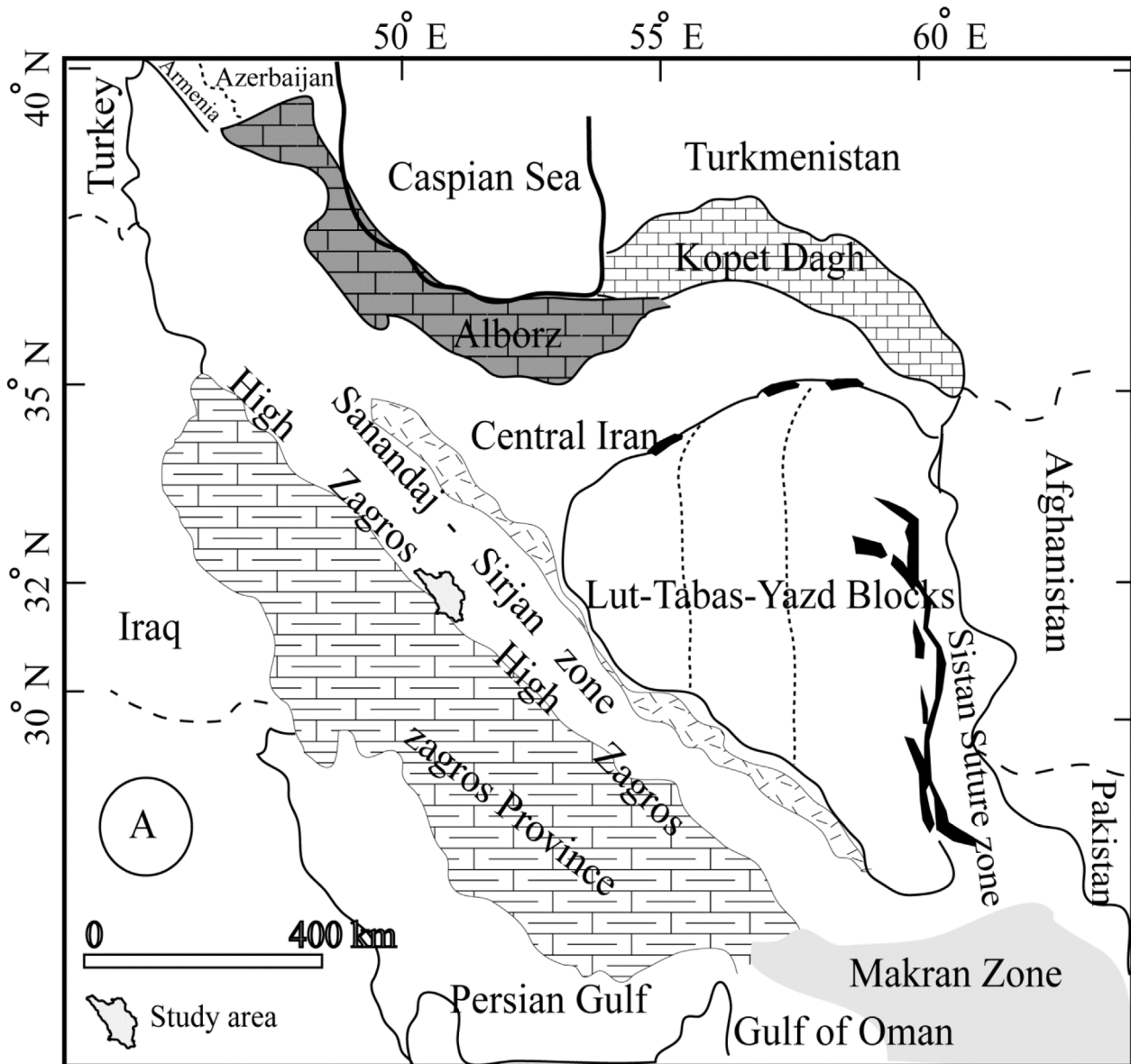


Fig. 1. Iran map showing the different geological zones of Iran (Alavi, 2004).

study area (Kuh-e- Soukhteh and North Gahrou sections) is exposed on the roadside in the Gahrou area (southwest Shahrekord) and located in sub-zones Z2b of the structural division of Chahar-mahal Bakhtiari province. Three groups of rock units with different geological ages are represented on the geological map of Shahrekord. The first group consists of a succession of Cretaceous *Orbitolina*-bearing limestone and *Globotruncana*-bearing argillaceous limestone and shale in the eastern and western parts of the map respectively. The second group corresponds to the Paleocene-Eocene conglomerate that crops out on the western banks of Choghakhor lake and in the northern part of the map. Finally, the third group consists of Eocene limestone, shale, and marl spread over much of the geological map of the region. The third group was the object of the detailed stratigraphic and paleontological work presented in this article.

5 Lithostratigraphy

In the study area, the Jahrum Formation consists of three main lithologies: limestone, marl, and dolomitic limestone (dolostone) based on field observation.

5.1 Kuh-e- Soukhteh Section

About 80 samples have been collected from layer 1 to layer 80, over a thickness of 157 m. The index "As" represents the Kuh-e- Soukhteh Section (Fig. 3). The six lithological units of the Jahrum Formation are described as follows:

- Unit 1 is about 52.5 m thick and extends from the horizon (bed) 1 to horizon (bed) 34 in stratigraphic order. This unit

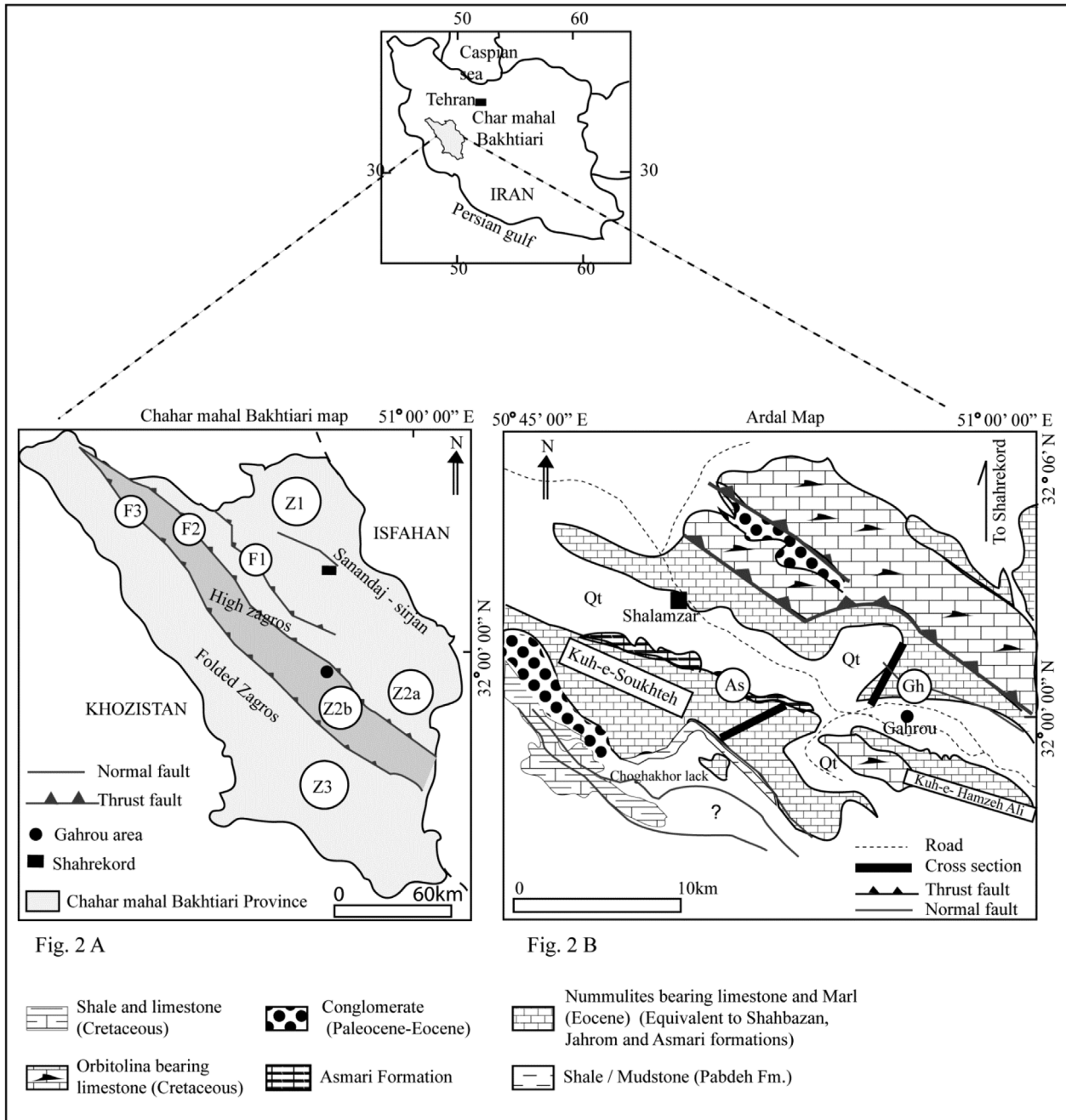


Fig. 2. (A) Location of the study area in the High Zagros on the Chaharmahal Bakhtiari Province (Zahedi and Rahmati Ilkhechi, 2006); (B) Location of the study area in Ardal geological map (1:250 000).

consists of a sedimentary succession of gray argillaceous limestone, thin layers of green marl, dolostone, and thin dolomitic limestone. These carbonate facies consist of mudstone, dolostone, intraclast packstone, miliolid-pellet wackestone, etc.

- Unit 2 immediately overlies Unit 1. It is 10 m thick and extends from bed 35 to bed 40. It mainly consists of medium bedded to thin-bedded gray limestone with intercalation of argillaceous limestone. The carbonate facies is bioclastic grainstone and *Macetadiscus*-miliolid-pellet wackestone.

- Unit 3, 38.5 m thick, extends from bed 40 to bed 56. It is mainly composed of medium to thick-bedded limestones. The carbonate facies is *Macetadiscus*-miliolid-pellet wackestone, conical porcellaneous-agglutinated foraminifera-miliolid wackestone, and intraclast packstone.
- Unit 4 consists of thin layers of dolomitic limestone, dolostone, and intercalation of limestone. It is 41 m thick and extends from bed 57 to bed 74. The carbonate facies is dolomitic wackestone and conical porcellaneous-agglutinated foraminifera-miliolid wackestone.

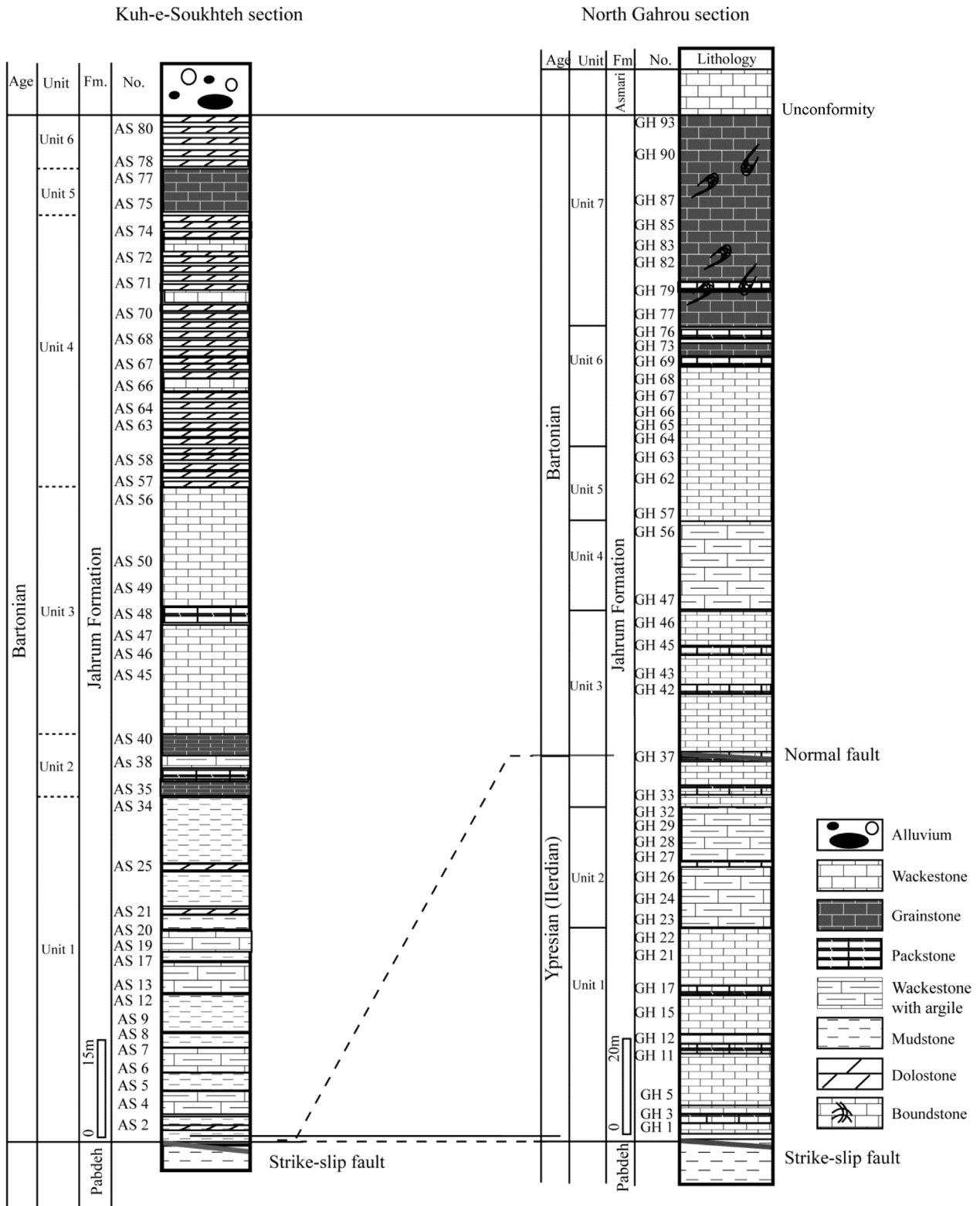


Fig. 3. Correlation between Kuh-e- Soukhteh and North Gahrou columnar sections showing the different lithological units in the study area.

- Unit 5, 7.5 m thick, is composed of medium bedded limestones. It is exposed in the interval between bed 75 and bed 77. The carbonate facies is bioclastic grainstone
- Unit 6, 7.5 m thick, extends from bed 78 to bed 80. It is composed of gray to cream medium to thin-bedded dolostone and dolomitic limestone. The carbonate facies is dolomitic wackestone.

5.2 North Gahrou Section

About 93 samples have been collected from this section 215 m thick, which consists of 93 individual beds. The index “GH” represents the Gahrou area (Fig. 3). Seven lithological units have been identified in the field from bottom to top:

- Unit 1, 45 m thick, displays medium layers of gray limestone and thin layers of cream limestone. It extends from bed GH 1 to bed GH 22. The carbonate facies consist of large hyaline foraminifera wackestone and packstone with a variety of benthic foraminiferal fauna.
- Unit 2 consists of cream argillaceous limestone, and gray thin-bedded limestone. It extends from bed GH 23 to bed GH 36. It is 34 m thick. Most of the biota are small *Nummulites* Lamarck and thin layer *Assilina* d’Orbigny. They are mainly composed of small hyaline foraminifera wackestone and packstone facies.
- Unit 3 consists of an alternation of medium to thick layers of cream and gray limestone. This unit extends from bed GH 37 to bed GH 46 and is mainly composed of large hyaline foraminifera wackestone and packstone. This unit is 33 m thick.
- Unit 4 consists of thin layers of gray argillaceous limestone. It is exposed in the interval between bed GH 47 to bed GH 56. This unit is 19 m thick.
- Unit 5, 17 m thick, consists of medium to thick layers of cream limestone with many coarse-grained bioclasts. It is mainly composed of porcellaneous foraminifera wackestone facies and is exposed in the interval between bed GH 57 to bed GH 63.
- Unit 6 consists of a succession of thin layers of gray to cream limestone. It is mainly textured as *Alveolina*-bioclast-pellet wackestone to grainstone facies. This unit is 25 m thick and extends from bed GH 64 to bed GH 76.
- Unit 7, 42 m thick, consists of cream limestone with many coarse-grained bioclasts such as *Gypsina* Carter. It is mainly composed of *Gypsina*-lump-bioclast grainstone with inter-layers of bioclast-intraclast packstone facies. This unit extends from bed GH 77 to GH 93.

6 Microfacies

According to Burchette and Wright (1992), carbonate ramp environments can be divided into three parts: 1) the internal ramp between the upper part of the coastal surface and the regular surface of the fair-weather wave base, which is affected by the turbulence of waves; 2) the intermediate ramp between the fair-weather wave base and storm-wave base along with the displacement of the sediment during the flood. The water depth varies from a few tens of meters to 100 to 200 m and; 3) the external ramp between underwater effect lines to deep basin. According to the study of about 170 rock samples, eight facies were identified and are described hereafter (Figs. 4 and 5).

6.1 Kuh-e- Soukhteh Section

6.1.1 Tidal flat

Mudstone Facies (Pl. 1, fig. J)

It consists of light gray argillaceous micritic limestone that contains rare small porcellaneous foraminifera, rare rotaliids and pellets, and in places shows fenestral fabric. In this type of facies microcrystalline calcite is widespread and micritization is controlled by biological and chemical factors. The occurrence of small and scattered porcellaneous foraminifera in the mud-supported facies (micritic textures) represents a near-shore environment (littoral zone) with low energy (Buxton and Pedley, 1989; Romero *et al.*, 2002).

Dolostone/dolomitic limestone Facies (Pl. 1, fig. K)

This facies consists of yellow to grey thin-bedded, finely crystalline, homogeneous but in places laminated dolomite. As a result of dolomitization, fossil fragments such as miliolids, rotaliids, and small bivalves faded and disappeared so that it is almost impossible to identify them. The dolomite grains are small and rhomboidal in shape. The dolomite is diagenetically recrystallized to coarser crystals. Vuggy porosities are also abundant in dolostone. This dolostone facies can be compared to dolo-mudstone facies of the Jahrum Formation from the Do Kuhak region in the Fars area of south Iran (Babazadeh and Pazooki Ranginlou, 2015).

6.1.2 Inner ramp (Lagoon)

– Miliolid–pellet wackestone (Pl. 1, fig. L)

This type of facies is dominated by pellet and small miliolids. It is characterized by the presence of micritic limestone, micrite grains, and small porcellaneous foraminifera. The peloids are structureless, spherical, ellipsoidal, and subrounded micritic grains. They are mostly well preserved and show weak to moderate sorting. Subordinate *Valvulina* sp. and bivalve fragments are present. This facies is equivalent to that of the Kras Plateau in southwest Slovenia (Zamagni *et al.*, 2008) and the Campo section in Spain (Rasser *et al.*, 2005).

– Macetadiscus-miliolid-pellet wackestone (Pl. 1, figs. A and M)

This yellow medium-bedded limestone contains miliolids, micritic pellets, and *Macetadiscus* Hottinger, Serra-Kiel and Gallardo-Garcia similar to the previous one except for the presence of *Macetadiscus* Hottinger, Serra-Kiel and Gallardo-Garcia. This facies shows a lateral paleoenvironmental relationship with the miliolid-pellet wackestone facies. The subordinate fauna consists of conical agglutinated foraminifera (*Coskinolina*) with rare small rotaliids and without *Alveolina* d’Orbigny. This facies is presented for the first time in the Zagros Mountains.

– Conical porcellaneous-agglutinated foraminifera-miliolid wackestone (Pl. 1, fig. Q; Pl. 2, fig. A)

This facies has a widespread distribution in this region and occurs in the middle part of the columnar section. It consists of dark grey micritic limestone containing flattened and conical porcellaneous- agglutinated foraminifera (20–30%), and small miliolids (40–50%). The other subordinate bioclasts (bivalves and gastropods) account for 10–20%.

Kuh-e-Soukhteh section

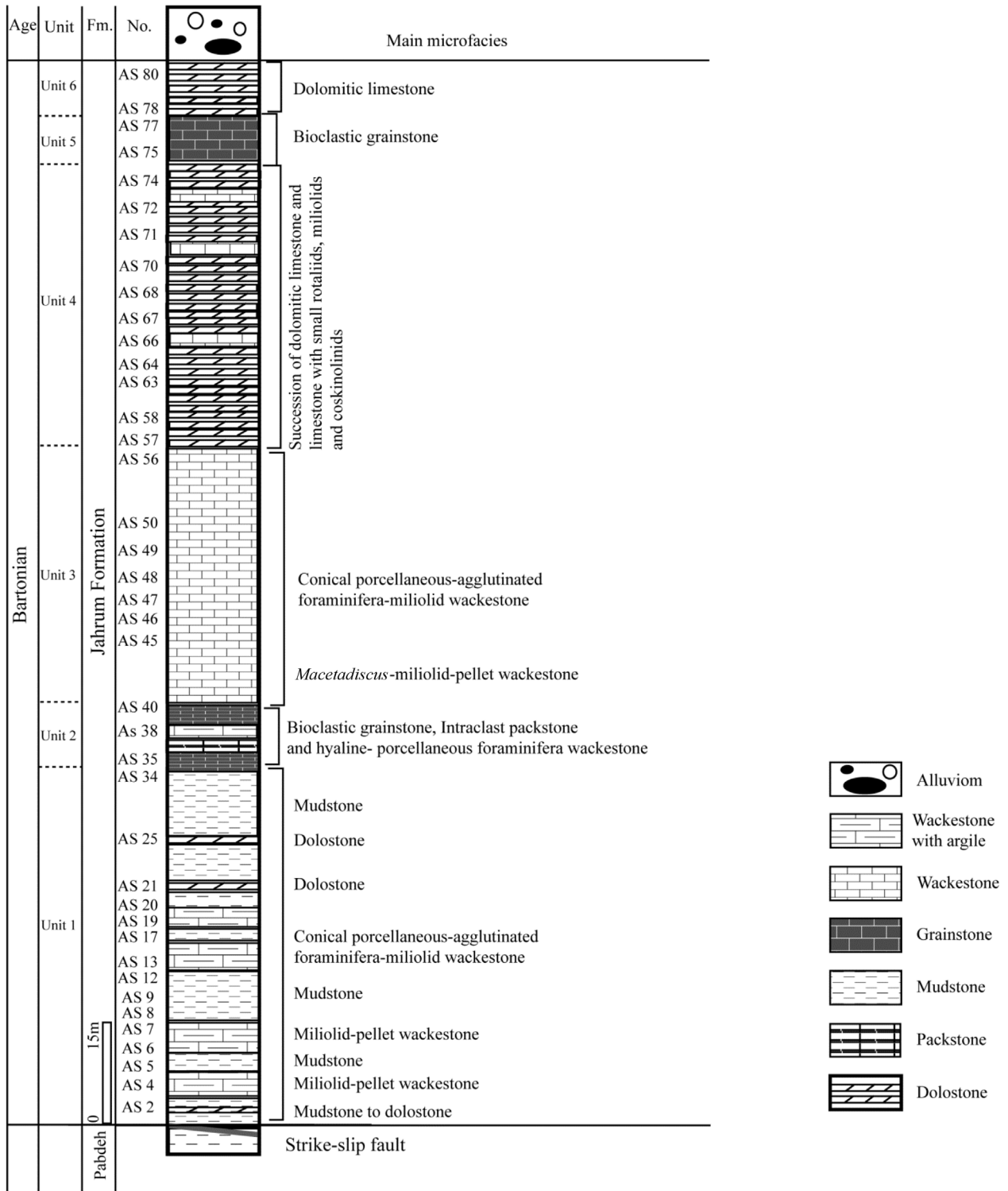


Fig. 4. Distribution of main microfacies in the Kuh-e- Soukhteh columnar section.

North Gahrou section

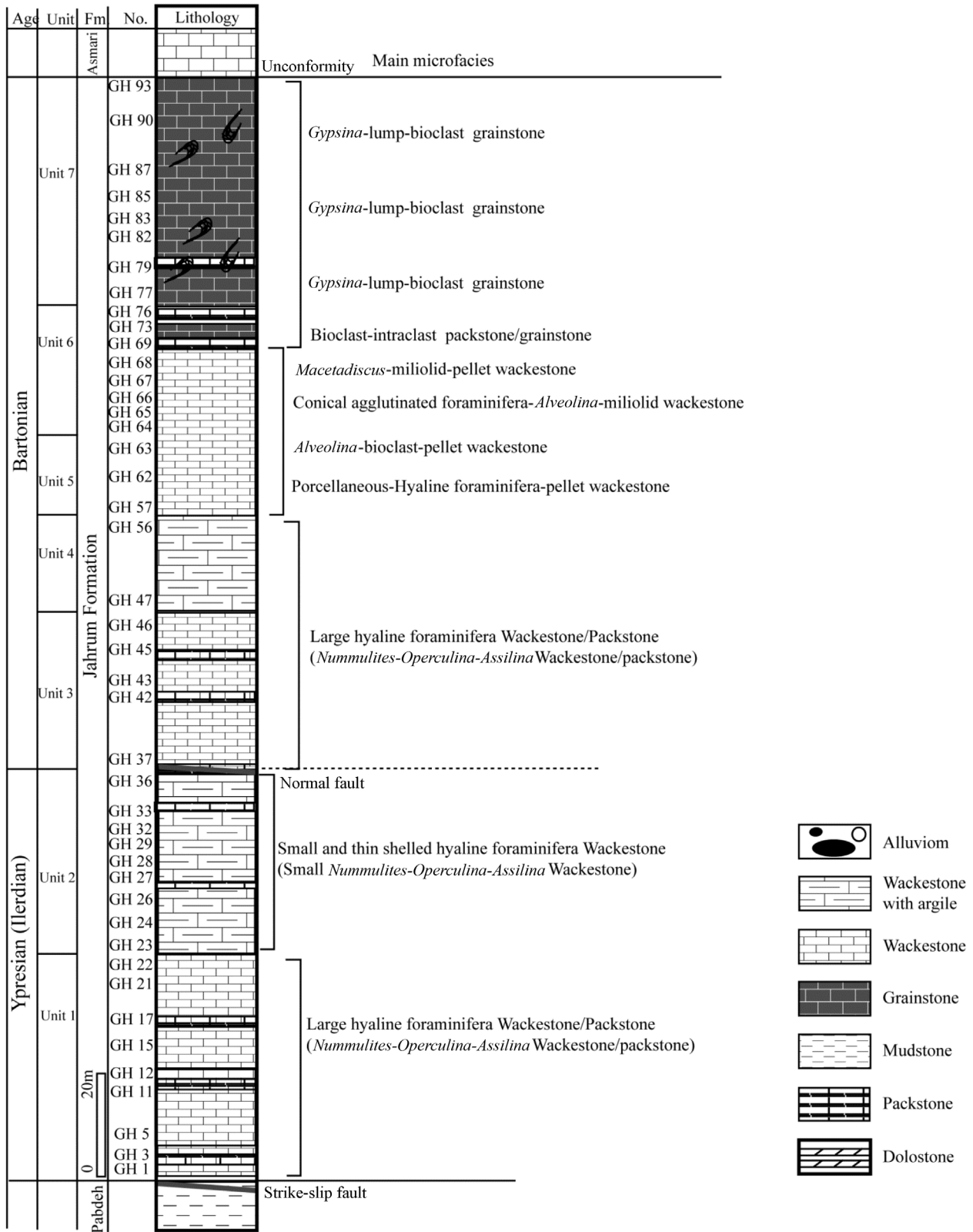


Fig. 5. Distribution of main microfacies in the North Gahrou columnar section.

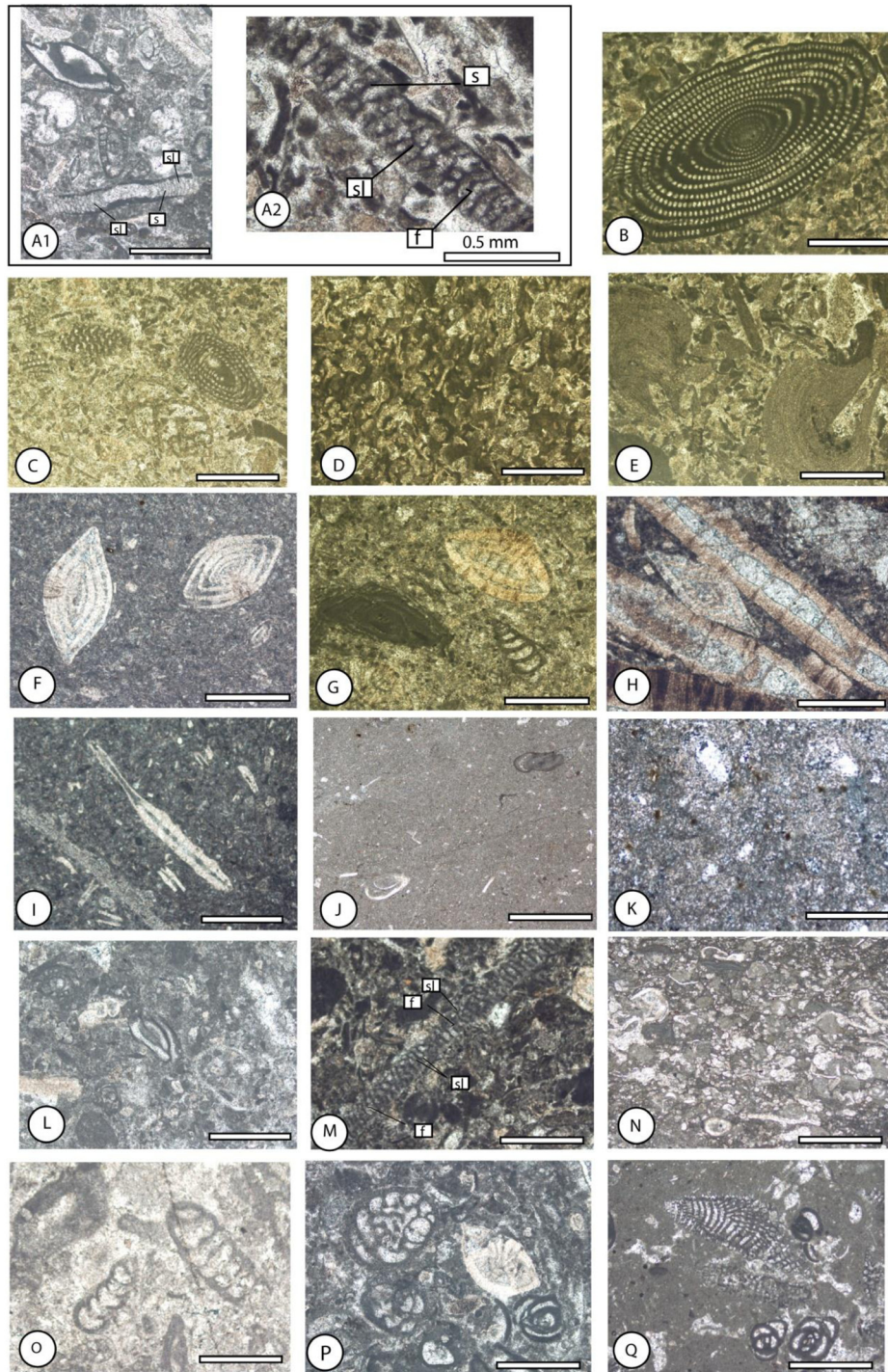


Plate 1. Figs. A: *Macetadiscus*-miliolid-Pellet wackestone, A1: Kuh-e- Soukhteh section, As 45 and A2: Gahrou section, GH 62; Fig. B: *Alveolina*-pellet wackestone, Gahrou section, GH 63; Fig. C: *Alveolina*-bioclast-pellet wackestone/grainstone, Gahrou section, GH 72; Fig. D: Bioclast-intraclast packstone/grainstone, Gahrou section, GH 76; Fig. E: *Gypsina*-lump- bioclast grainstone, Gahrou section, GH 77; Fig. F: Hyaline foraminifera (*Nummulites* sp.) wackestone, Gahrou section, GH 25; Fig. G: Porcellaneous-hyaline-foraminifera- Pellet wackestone, Gahrou section, GH 58; Fig. H: Large hyaline foraminifera (*Assilina* sp.) wackestone/packstone, Gahrou section, GH 1; Fig. I: Large hyaline foraminifera [*Operculina* cf. *patalensis* (Davies)] wackestone, Gahrou section, GH 5; Fig. J: Mudstone with miliolids, Kuh-e- Soukhteh section, As 11; Fig. K: Dolostone or dolomitic limestone without fossils, Kuh-e- Soukhteh section, As 26; Fig. L: Miliolid-Pellet wackestone, Kuh-e- Soukhteh section, As 40; Fig. M: *Macetadiscus*-miliolid-Pellet wackestone, Kuh-e- Soukhteh section, As 41; Fig. N: Intraclast packstone with gastropods fragments, Kuh-e- Soukhteh section, As 19; Fig. O: Bioclastic grainstone, Kuh-e- Soukhteh section, As 75; Fig. P: Hyaline-porcellaneous foraminifera wackestone, Kuh-e- Soukhteh section, As 38; Fig. Q: Conical porcellaneous foraminifera-miliolid wackestone, Kuh-e- Soukhteh section, As 14; All scale bars = 1 mm, except A2 = 0.5 mm.

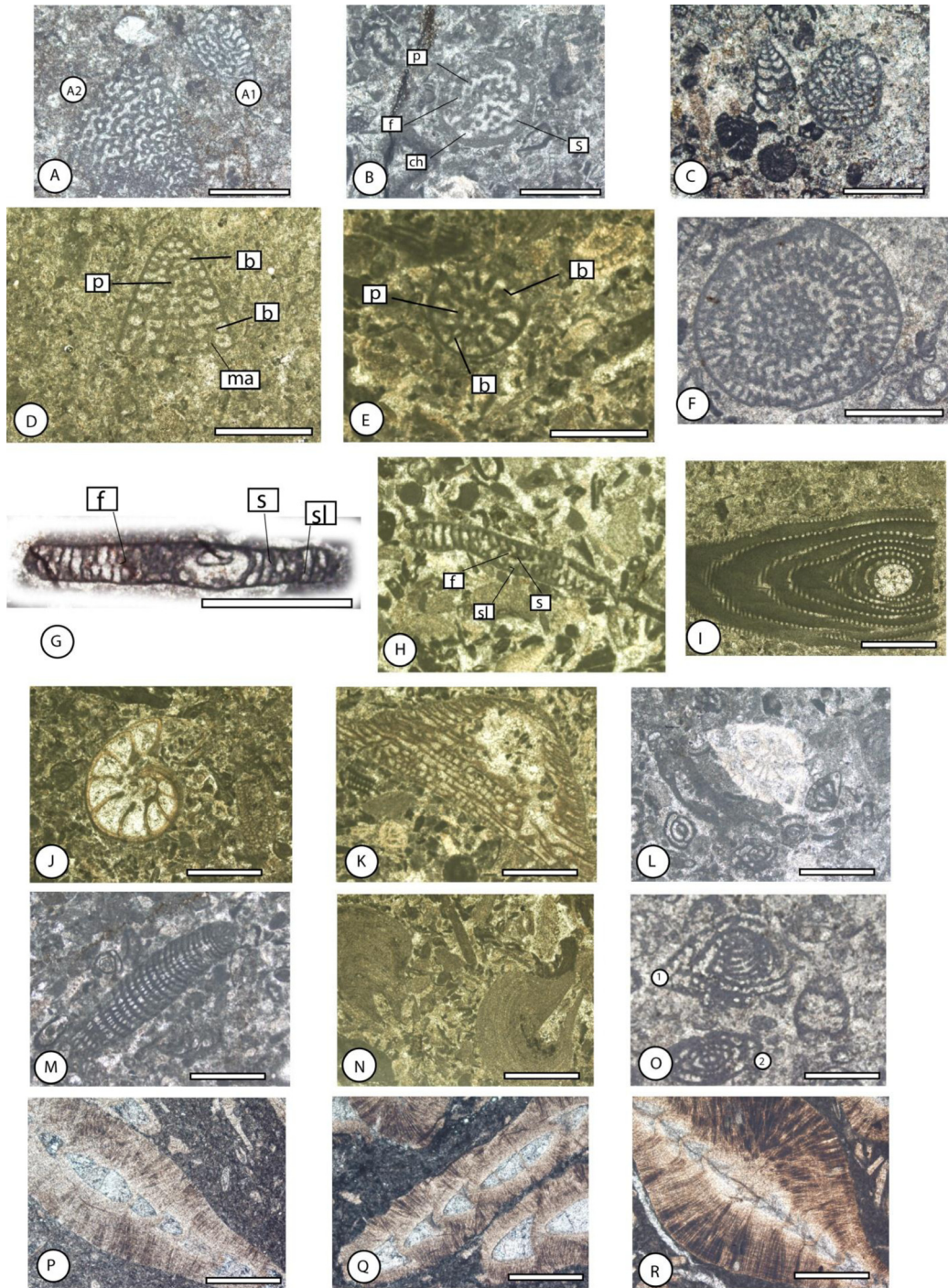


Plate 2. Fig. A: A1) *Coskinolina perpera* Hottinger and Drobne, axial section, Kuh-e- Soukhteh section, As 46, A2) *Coskinolina liburnica* Stache, axial section, As 46; Fig. B: *Coskinolina perpera* Hottinger and Drobne, equatorial section, Kuh-e- Soukhteh section, As 38; Fig. C: *Coskinolina perpera* Hottinger and Drobne, oblique section, Kuh-e- Soukhteh section, As 80; Fig. D: *Daviesiconus* cf. *balsilliei* (Davies), subaxial section, Gahrou section, GH 64; Fig. E: *Daviesiconus* cf. *balsilliei* (Davies), equatorial section, Gahrou section, GH 63. Fig. F: *Barattolites* cf. *trentinarensis* Vecchio and Hottinger equatorial section, Kuh-e- Soukhteh section, As 80; Fig. G: *Macetadiscus* cf. *incolumnatus* Hottinger, subaxial section, Kuh-e- Soukhteh section, As 41; Fig. H: *Alveolina* cf. *fusiformis* Stache, axial section, Gahrou section, GH 60; Fig. I: *Gyroidinella magna* Le Calvez, equatorial section, Gahrou section, GH 69; Fig. K: *Fabiania cassis* (Oppenheim), axial section, Gahrou section, GH 63; Fig. L: *Medocia blayensis* Parvati, subaxial section, Kuh-e- Soukhteh section, As 42; Fig. M: *Rhabdorites malatyaensis* (Sirel), subaxial section, Kuh-e- Soukhteh section, As 42; Fig. N: *Gypsina marianensis* Hanzawa, axial section, Gahrou section, GH 77; Fig. O1: *Archaias operculiniformis* Henson, oblique (nearly axial section), Kuh-e- Soukhteh section, As 77, Fig. O2: *Penarchaias glynnjonesi* (Henson), transverse section parallel to the axis of coiling, Kuh-e- Soukhteh section, As 77; Fig. P: *Assilina* cf. *laminosa* (Gill), axial section, Gahrou section, GH 1; Fig. Q: *Assilina* cf. *granulosa* (d'Archiac), axial section, Gahrou section, GH 38; Fig. R: *Assilina* cf. *khorrassanica* (Rahaghi), subaxial section, Gahrou section, GH 3, Scale bars: 1 mm. b: beam, ch: chamber, f: foramen, p: pillar, s: septum, sl: septulum, ma: marginal aperture.

6.1.3 Middle ramp (shoal)

– Intraclast packstone (Pl. 1, fig. N)

This facies consists of thin to medium bedded grey limestone and appears as medium-grained (1–2 mm) calcarenites in the field. The intraclasts (up to 50%) and peloids (10–20%) are the most abundant components of this facies. Smaller foraminifera (miliolids) and other subordinate bioclasts account for 5–20%. The intraclasts consist of silt to sand-sized carbonate grains showing smooth or sub-angular edges displaced and re-deposited by currents within the micritic matrix.

– Bioclastic grainstone (Pl. 1, fig. O)

This facies is a medium bedded yellow to grey finely crystalline limestone. The dominant bioclasts (benthic foraminifera), as well as bivalve and gastropod fragments, are cemented by calcite. The presence of broken and abraded large benthic foraminifera (*Coskinolina*, *Macetadiscus*, *Haymanella*, etc.) and rounded rotaliids (*Medocia* and *Rotalia*) in sparitic cement suggest shallow-water sedimentation in low-relief shoal environment. This facies accumulated in a shoal close to sea level.

6.1.4 Middle ramp (back and fore shoal)

– Hyaline-porcellaneous foraminifera wackestone (Pl. 1, fig. P)

This facies is a yellow to grey thin-bedded limestone with a micritic matrix. The components are dominated by porcellaneous or imperforate (e.g., *Haymanella*) and hyaline or perforate foraminifera (semi-conical rotaliids, e.g., *Rotaliconus* and *Medocia*), the other components such as agglutinated foraminifera and bivalve fragments are subordinate.

6.2 North Gahrou Section

In this section, eight major facies defined by biota (fossil) and abiotic (non-fossil) components are represented.

6.2.1 Inner ramp (Lagoon)

– *Macetadiscus*-miliolid-pellet wackestone (Pl. 1, fig. A)

This facies consists of grey micritic limestone, in which pellets are the most abundant components (up to 40%), followed by miliolids and *Macetadiscus* Hottinger, Serra-Kiel & Gallardo-García. This facies is comparable to the facies number four of the Kuh-e- Soukhteh. The presence of *Macetadiscus* Hottinger, Serra-Kiel & Gallardo-García suggests relatively shallower water than *Alveolina* facies. This facies has a lateral paleoenvironmental relationship with the *Alveolina*-pellet wackestone facies.

– Conical agglutinated foraminifera-*Alveolina*-pellet wackestone (Pl. 1, fig. B)

This facies comprises yellow to grey thin-bedded limestone. The main components are pellets (up to 45%) and *Alveolina* d'Orbigny (15–35%). Subordinate components are miliolid smaller foraminifera, *Barattolites* Hottinger, Serra-Kiel & Gallardo-García and a few rotaliids. The

Alveolina d'Orbigny are important elements in the Lower and Middle Eocene shallow-water deposits. They are also abundant in the lagoon or enclosures behind the back shoal as well as in the shoal and are found in relatively deeper water than *Orbitolites* Lamarck. This facies is comparable to that of the Birjand region in east Iran (Babazadeh, 2010; Babazadeh and Alavi, 2013).

– *Alveolina*-bioclast-pellet wackestone (Pl. 1, fig. C)

This facies consists of grey medium bedded limestones. The *Alveolina* d'Orbigny and bioclasts (up to 50%) are in equal abundance and are bounded by calcite cement. All other components such as miliolids, *Macetadiscus* Hottinger, Serra-Kiel & Gallardo-García, and conical agglutinated foraminifera are subordinate and distributed irregularly among the samples. Pellets and bivalve fragments are less abundant. The presence of *Alveolina* d'Orbigny indicates a lagoonal condition and occurred in a sheltered depositional environment at a protected shelf (Hottinger, 1983; Beavington-Penney and Racey, 2004).

6.2.2 Shoal

– Bioclast-intraclast packstone/grainstone (Pl. 1, fig. D)

This facies consists of yellow medium bedded limestone with coarse crystalline calcite. The intraclasts (up to 80%) and bioclasts (10%) are the most abundant components in this facies. The miliolid smaller foraminifera and pellets account for 5–10%. Based on the presence of micritic texture and calcite cement, this facies can change from packstone to grainstone. Due to the low abundance of micrite and dominance of bioclasts, this facies represents higher energy than the previous facies.

– *Gypsina*-lump-bioclast grainstone (Pl. 1, fig. E)

In this facies, the main components are bioclasts as well as *Gypsina* Carter and lumps (up to 70%). Subordinate components are small miliolids, a few agglutinated foraminifera (*Barattolites* sp.), and echinoid fragments. Although this facies separates the lagoon from the open sea, it represents a high-energy environment as testified by the abundance of intraclasts and bioclasts and the absence of micrite. This facies is recognized for the first time in the Zagros Mountains.

6.2.3 Back shoal

– Small and thin-shelled hyaline foraminifera wackestone (Pl. 1, fig. F)

This facies comprises yellow to grey thin-bedded limestones with small *Nummulites* Lamarck and small *Operculina* d'Orbigny as main components. The small *Nummulites* Lamarck are robust and ovate whilst the small *Operculina* d'Orbigny are thin and elongated. The small and robust *Nummulites* Lamarck occurred in a broad range of open marine environments on both ramp and shelves and are generally absent from more restricted waters.

– Porcellaneous-Hyaline foraminifera-pellet wackestone (Pl. 1, fig. G)

This facies consists of grey medium bedded limestone, which contains porcellaneous foraminifera (*Alveolina*) outnumbering hyaline foraminifera (small *Nummulites*). It reflects an offshore transport of porcellaneous forms into the hyaline

foraminiferal facies. The bioclasts and pellets are more abundant in the micritic matrix. All other components such as agglutinated conical foraminifera are subordinate and distributed irregularly among the samples. This facies is comparable with the Do Kuhak region in the Fars area of south Iran (Babazadeh and Pazooki Ranginlou, 2015).

6.2.4 Fore shoal

– Large hyaline foraminifera wackestone/packstone (Pl. 1, figs. H–I)

The major fauna of this facies is constituted by large hyaline thin to thick-shelled foraminifera. The densely packed nummulitid tests (*Operculina* and *Assilina*) account for over 70% of the rock volume. Other components are *Discocyclus* Gumbel and small *Nummulites* Lamarck. This facies is comparable with MFT4 of the Kaboudeh section in east Iran (Babazadeh, 2010).

7 Interpretation and depositional environment

In the North Gahrou Section, during the Early Eocene (Ilerdian), the large hyaline foraminifera wackestone is repeated twice throughout the columnar section and occupies the basal and middle part of the study section. This facies indicates low-energy depositional condition in the proximal outer ramp environment due to the presence of thin and elongated shells of *Operculina* d'Orbigny and *Assilina* d'Orbigny (Racey, 2001; Beavington-Penney *et al.*, 2006). It is followed up section by small hyaline foraminifera wackestone and packstone, indicating somewhat shallower water depths than the former facies, interpreted as the external part of the middle ramp.

During the Bartonian, large hyaline foraminifera wackestone, overlying the succession of Early Eocene deposits, records the reestablishment of the initial ramp environment. It is overlain by shallow water deposits with porcellaneous-hyaline foraminifera-pellet wackestone facies indicating a shallowing upward trend in the fore shoal environment. It was followed by different shallow-water facies such as *Alveolina*-bioclast-pellet wackestone, conical agglutinated foraminifera-*Alveolina*-pellet wackestone and *Macetadiscus*-miliolid-pellet wackestone. They are equivalent to the inner ramp facies of the Kuh-e- Soukhteh section and occurred in the middle part of the study section (units 3, 4, 5 and 6). The bioclast-intraclast packstone/grainstone and *Gypsina*-lump-bioclast grainstone occupy the upper part of the study section. They record the shoal environment in the middle ramp setting and represent a high-energy deposit above the fair-weather wave base. The lime muds are swept from the grainstone and the bioclasts and intraclast are abundant in the shoal environment.

In the Kuh-e- Soukhteh section, during the Bartonian, the facies of mudstone with intercalation of dolomitic limestone consists of small porcellaneous foraminifera (miliolids), rare small hyaline perforate foraminifera (rotaliids), scarce pellets and thin shells of bivalves. This type of association represents a tidal flat in the coastal plain. It gradationally passes over to wackestone with the incorporation of more bioclasts in

places. Episodic currents washed peloids onto the lagoonal environment and led to the formation of miliolid-pellet wackestone. Back-stepping is proved by the appearance of the wackestone containing conical porcellaneous forms (spiro-liniform such as *Neorhipidionina* Hottinger), agglutinated forms, and small miliolids. These facies exhibit an alternation of thin layers of mudstone and relatively thicker wackestone beds at the lower part of the section, which typically represent a shallow water environment in the subtidal lagoon to back shoal setting. The transition from tidal flats to lagoonal environment occurred in a shallow subtidal environment. The dominance of micritic sediments indicates a low-energy depositional setting. Further up in the section, the bioclastic grainstone with intraclast packstone and hyaline- porcellaneous foraminifera wackestone can be seen. The intraclast and abraded fauna abound in the shoal setting. These facies typically represent shoal and marginal shoal and extend from the inner ramp to the proximal middle ramp setting, below normal wave agitation depth but occasionally affected by storms. They are followed by the *Macetadiscus*-miliolid-pellet wackestone and conical porcellaneous-agglutinated-miliolid foraminifera with some rotaliids in the middle part of the section. This part is similar to the lower part of the section, due to the presence of abundant porcellaneous foraminifera. The uppermost part of the section consists of a succession of dolomitic limestone and limestone with subordinate foraminifera (miliolids, small rotaliids, and coskinolinids) associated with inter-bedded of bioclastic grainstone.

8 Biostratigraphy

The Jahrum Formation is rich in larger benthic foraminifera which were used for establishing the biostratigraphic zonation. This formation, which represents marine strata in the Shahrekord region, was rarely studied and poorly documented. Based on larger benthic foraminifera, the Eocene Assemblage Zones of Jahrum Formation were established by James and Wynd (1965), Adams and Bourgeois (1967), Hottinger (2007), and in the study area (Figs. 6A and 6B). In the current study 44 species of benthic foraminifera were identified for the first time. The benthic foraminiferal fauna were collected from the gray to cream limestone and argillaceous limestone present throughout the two studied sections (North Gahrou and Kuh-e-Soukhteh sections) (Figs. 5 and 6).

8.1 Assemblage Zones

Three assemblage zones were identified; Assemblage Zone A and Assemblage Zone B, which occurred in the North Gahrou section, and Assemblage Zone C represented in the Kuh-e- Soukhteh section. Selected larger benthic foraminifera are figured in Plates 2 and 3.

8.1.1 Assemblage Zone A (Fig. 7)

This zone is exposed in the lower part of the section and extends from bed GH 1 to bed GH 37. It is characterized by the presence of the following species: *Assilina* cf. *khorrassanica* (Rahaghi), *Assilina* cf. *laminosa* (Gill), *Assilina* cf. *granulosa* (d'Archiac), *Assilina* cf. *subspinosa* (Davies), *Operculina* cf. *patalensis* (Davies), *Nummulites globulus*

A

Formation	Age	Wynd (1965)	Adams & Bourgeois (1967)	
	Jahrum Formation	Late Eocene	<i>Chapmanina-Pellatispira-Baculogypsinoides</i> Assemblage Zone (Zone 53)	<i>Nummulites</i> spp.- <i>Discocyclina</i> spp. Assemblage Zone
		Middle Eocene	<i>Nummulites-Alveolina</i> Assemblage Subzone (51)	<i>Coskinolina-Rhapydionina</i> Assemblage Zone
			<i>Dictyoconus-Coskinolina-Orbitolites complanatus</i> Assemblage Subzone (50)	
			Linderina Subzone (49)	
Somalina Subzone (48)				
E. Eocene	<i>Opertorbitolites</i> Zone (44)			
Paleocene	<i>Miscellanea-Kathina</i> Assemblage Zone (Zone 43)			

B

Biozones (Serra-Kiel et al. 1998)	Fars area (Hottinger 2007)	In this study	
		North Gahrou section	Kuh-e-Soukhteh section
Bartonian SBZ 17 - 18	<i>Globoreticulina iranica</i> <i>Austrotrillina paucialveolata</i> <i>Austrotrillina eocaenica</i> <i>Neorhapydionina spiralis</i> <i>Hymanella huberi</i> <i>Praerhapydionina delicata</i> <i>Rhabdorites malatyaensis</i> <i>Neotaberina neaniconica</i> <i>Orbitolites minimus</i> <i>Penarchaias glymijonesi</i> <i>Archaias operculiniformis</i> <i>Archaias diyarbakirensis</i> <i>Coskinolina perpera</i> <i>Coskinolina liburnica</i> <i>Dictyoconus indicus</i> <i>Medocia blayensis</i> <i>Rotalicomus persicus</i>	Assemblage B <i>Nummulites</i> cf. <i>perforatus</i> <i>Nummulites ptukhiani</i> <i>Gyroidinella magna</i> <i>Alveolina</i> cf. <i>fusiformis</i> <i>Barattolites</i> sp. <i>Asterigerina rotula</i> <i>Gypsina marianensis</i> <i>Fabiania cassis</i> <i>Alveolina elliptica</i> <i>Nummulites malatyaensis</i> <i>Daviesicomus</i> cf. <i>balsilliei</i>	Assemblage C <i>Austrotrillina eocaenica</i> <i>Neorhapydionina spiralis</i> <i>Hymanella huberi</i> <i>Praerhapydionina delicata</i> <i>Rhabdorites malatyaensis</i> <i>Macetadiscus</i> cf. <i>incolumnatus</i> <i>Nurdanella boluensis</i> <i>Archaias operculiniformis</i> <i>Penarchaias glymijonesi</i> <i>Coskinolina perpera</i> <i>Coskinolina liburnica</i> <i>Medocia blayensis</i> <i>Rotalicomus persicus</i> <i>Barattolites</i> sp.
	Ypresian (Ilerdian) SBZ 8	Assemblage A <i>Assilina</i> cf. <i>khorrassanica</i> <i>Assilina</i> cf. <i>laminosa</i> <i>Assilina</i> cf. <i>granulosa</i> <i>Assilina</i> cf. <i>subspinosa</i> <i>Operculina</i> cf. <i>patalensis</i> <i>Nummulites atacicus</i> <i>Nummulites</i> cf. <i>fossulata</i> <i>Nummulites globulus</i>	

Fig. 6. (A) Benthic foraminifera biozones of Wynd (1965) and Adams and Bourgeois (1967); (B) Benthic foraminifera biozones of Hottinger (2007) and the study area.

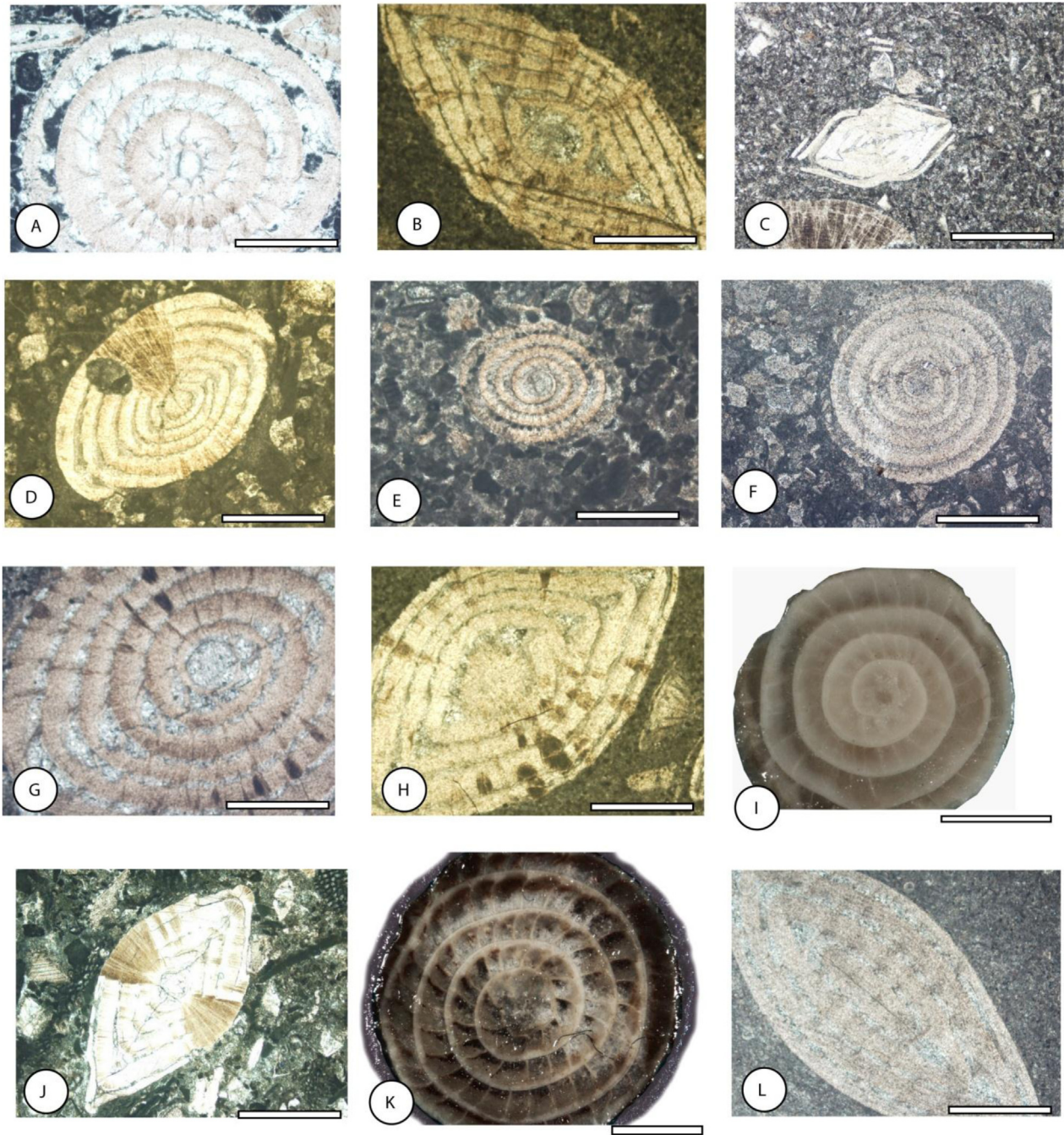


Plate 3. Fig. A: *Nummulites ptukhiani* Kacharava, equatorial section, Gahrou section, GH 51; Fig. B: *Nummulites ptukhiani* Kacharava, axial section, Gahrou section, GH 47; Fig. C: *Nummulites* cf. *fossulata* Cizancourt, axial section, Gahrou section, GH 11; Fig. D: *Nummulites malatyaensis* Sirel, axial section, Gahrou section, GH 90; Fig. E: *Nummulites* cf. *malatyaensis* Sirel, axial section, Gahrou section, GH 93; Fig. F: *Nummulites malatyaensis* Sirel, equatorial section, Gahrou section, GH 90; Fig. G: *Nummulites* cf. *perforatus* (de Montfort), equatorial section, Gahrou section, GH 37; Fig. H: *Nummulites* cf. *perforatus* (de Montfort), axial section, Gahrou section, GH 43; Fig. I: *Nummulites globulus* Leymerie, equatorial section, Gahrou section, GH 21; Fig. J: *Nummulites globulus* Leymerie, axial section, Gahrou section, GH 21; Fig. K: *Nummulites atacicus* Leymerie, equatorial section, Gahrou section, GH 25; Fig. L: *Nummulites atacicus* Leymerie, semi axial section, Gahrou section, GH 25. Scale bars: 1 mm.

Leymerie, *Nummulites atacicus* Leymerie, and *Nummulites cf. fossulata* de Cizancourt.

This zone was recognized in the lower part of the section and attributed to the Early Eocene (Ypresian). It is equivalent to the foraminiferal association of Lower Eocene deposits in Sahlabad Province (Sistan Suture Zone; east Iran) (Babazadeh, 2008, 2010), Eocene beds of Kohat Potowar Basin, and Punjab Salt Range in Pakistan as well (Akhtar and Butt, 1999; Mirza et al., 2005; Ahmad et al., 2014). This zone can be correlated with SBZ 8 of Serra-Kiel et al. (1998).

Stratigraphic range: Early Eocene (Ypresian: Ilerdian).

8.1.2 Assemblage Zone B (Fig. 7)

This zone is recognized in the upper part of the section and extended from bed GH38 to bed GH93. It has been characterized by an association of *Nummulites cf. perforatus* (de Montfort), *Nummulites ptukhiani* Kacharava, *Nummulites malatyensis* Sirel, *Alveolina cf. fusiformis* Stache, *Alveolina elliptica* (Sowerby), *Gyroidinella magna* Le Calvez, *Macetadiscus cf. incolumnatus* Hottinger, Serra-Kiel and Gallardo-Garcia, *Barattolites* sp., *Daviesiconus cf. balsilliei* (Davies), *Fabiania cassis* (Oppenheim), *Asterigerina rotula* (Kaufmann), *Gypsina marianensis* Hanzawa, *Europertia* sp., *Valvulina* sp., and miliolids.

This zone is recognized in the upper part of the section and assigned to the late Middle Eocene (Bartonian). This benthic assemblage is similar to that of the west Tethys (Serra-Kiel et al., 1998) and central Neo-Tethys realm (south, center, and east Turkey) (Sirel, 2003; Deveciler, 2010, 2013). This zone can be correlated with SBZ 17 & 18 of Serra-Kiel et al. (1998).

Stratigraphic range: late-Middle Eocene (Bartonian).

8.1.3 Assemblage Zone C (Fig. 8)

In the Kuh-e- Soukhteh section, one single assemblage zone appeared continuously from the base to the top. This zone consists of *Rhabdorites malatyensis* (Sirel), *Neorhipidionina spiralis* Hottinger, *Archaias operculiniformis* Henson, *Penarchaias glynnjonesi* (Henson), *Praerhapydionina delicate* Henson, *Haymanella huberi* (Henson), *Paraspirolina cf. gigantea* Fleury, *Spirolina cf. cylindracea* Lamarck, *Macetadiscus cf. incolumnatus* Hottinger, *Coskinolina perpera* Hottinger and Drobne, *Coskinolina liburnica* Stache, *Barattolites* sp., *Daviesiconus cf. balsilliei* (Davies), *Medocia blayensis* Parvati, *Rotaliconus persicus* Hottinger, *Rotalia* sp., *Nurdanella cf. boluensis* Ozgen, *Biloculina* sp., *Triloculina* sp., *Quinqueloculina* sp., and *Valvulina* sp. According to Hottinger (2007), Serra-Kiel et al. (2016) and Changaei et al. 2023 this association is the same as that of central Neo-Tethys (Fars area, south Iran; Shahrekord region, west Iran; Dhofar, Oman; Socotra Island, Yemen). The Assemblage Zone C is equivalent to the Assemblage Zone B. The biostratigraphic range of this assemblage may be correlated with SBZ 17 & 18 of Serra-Kiel et al. (1998).

Stratigraphic range: late-Middle Eocene (Bartonian).

9 Paleontological remarks

Among the reported benthic foraminifera, only the following taxa were selected for structural description and comparison.

Coskinolina perpera Hottinger and Drobne, *Daviesiconus cf. balsilliei* (Davies), *Barattolites* sp., *Macetadiscus cf. incolumnatus* Hottinger, Serra-Kiel and Gallardo-Garcia, *Nummulites globulus* Leymerie, *Nummulites atacicus* Leymerie, *Nummulites cf. fossulata* de Cizancourt, *Nummulites malatyensis* Sirel, *Nummulites cf. perforatus* (de Montfort), *Nummulites ptukhiani* Kacharava, *Assilina cf. laminosa* Gill, *Assilina cf. khorassanica* Rahaghi and *Assilina cf. granulosa* (d'Archiac).

The genus *Coskinolina* Stache is characterized by a thick agglutinated conical test with discontinuous pillars in the internal structure and without radial partitions (beams and intercalary beams) and rafters. The genus *Barattolites* Vecchio and Hottinger differs from *Coskinolina* Stache in the presence of beams and intercalary beams.

Coskinolina perpera Hottinger and Drobne (Pl. 2, figs. A–C) has a thicker wall than all other species of the same genus. The pillars show an irregular pattern and are loosely disposed of in the central part of the cone test. The sutures are depressed and the cone base is slightly convex. The genus *Daviesiconus* Hottinger and Drobne is close to the genus *Barattolites* Vecchio and Hottinger due to the trochospiral nepionic stage in both generations and simple exoskeleton but differs in the presence of marginal apertures, small trochospiral early growth stage and the absence of intercalary beams.

In our material, *Daviesiconus cf. balsilliei* (Davies) (Pl. 2, figs. D–E) has an axial cone diameter of 1.25 mm and the basal cone diameter of 1.1–1.25 mm in megalospheric form. The ratio between basal length and axial length (flattening index, Rb/a) is approximately 1. This specimen shows an isometric form and plots on the normal line of the flattening index diagram (Babazadeh 2022). It is similar to the specimens of *Daviesiconus balsilliei* (Davies) collected from former Yugoslavia (Hottinger and Drobne, 1980) but it differs from those of Oman and Yemen (Serra-Kiel et al., 2016) in the smaller size of the test.

The *Barattolites cf. trentinarensis* Vecchio and Hottinger (Pl. 2, fig. F) from the Iranian specimens (our material) has a larger size with respect to the *Barattolites trentinarensis* Vecchio and Hottinger from the Trentinara Formation of southern Italy.

The genus *Macetadiscus* Hottinger, Serra-Kiel, and Gallardo-Garcia was established by Serra-Kiel et al. (2016) and reported by Nafarih et al. (2019) from the Fars area in southern Iran. It is represented in this paper for the first time in the Shahrekord area. This genus is characterized by the porcellaneous flattened-discoidal test with two or three chambers without skeletal elements in nepionic stage (primary cyclic chambers), discontinuous septula in the annular chambers of the neanic stage, and the presence of foramina in lines with crosswise-oblique axes (Serra-Kiel et al., 2016). *Macetadiscus* Hottinger, Serra-Kiel, and Gallardo-Garcia differs from *Omanodiscus* Hottinger, Serra-Kiel, and Gallardo-Garcia by the presence of discontinuous septula in annular chambers and the absence of pillars. It is also distinguished from *Orbitolites* Lamarck, *Mardinella* Meriç and Coruh and *Azzarolina* Vicedo and Serra-Kiel by the presence of discontinuous septula in annular chambers and the absence of the septula in the primary cyclic chambers and the pillars respectively. The cyclic chambers of *Orbitolites* Lamarck are subdivided into numerous chamberlets by oblique septula

North Gahrou section

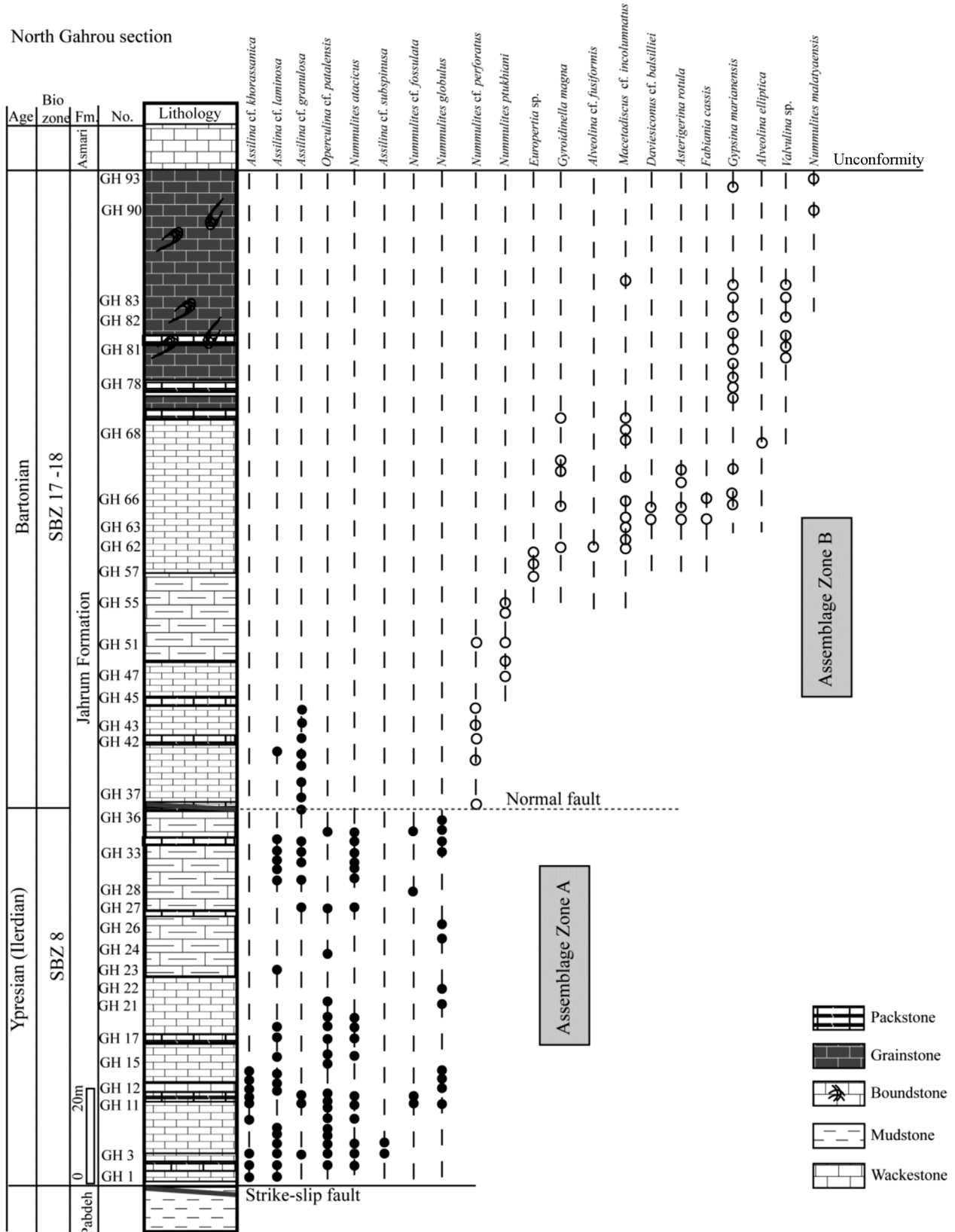


Fig. 7. Distribution of benthic foraminifera in the North Gahrou columnar section.

Kuh-e-Soukhteh section

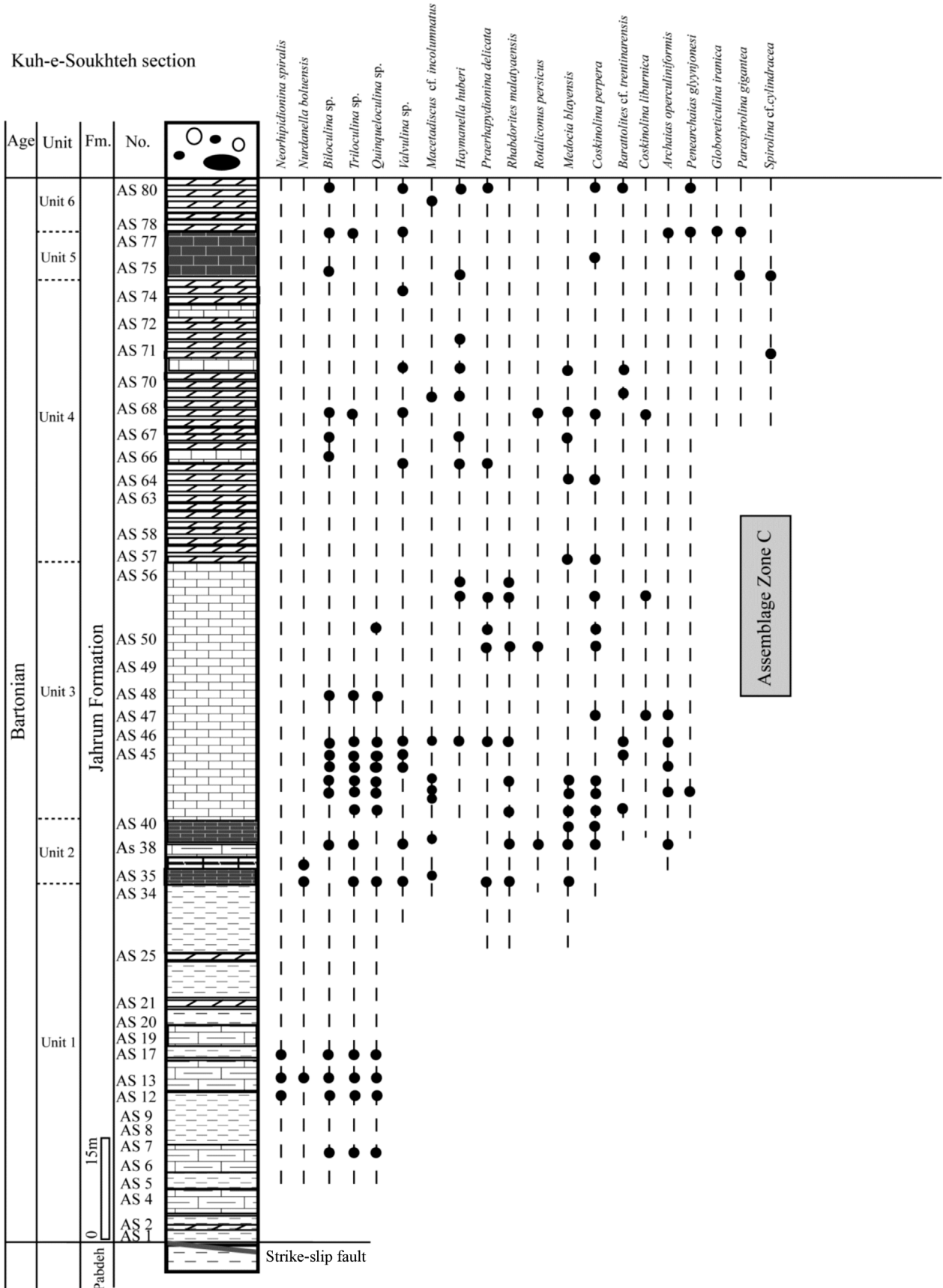


Fig. 8. Distribution of the benthic foraminifera in the Kuh-e- Soukhteh columnar section.

(partitions) unlike *Mardinella* Meriç and Coruh with septula perpendicular to the chamber walls.

In our samples, *Macetadiscus* cf. *incolumnatus* Hottinger, Serra-Kiel, and Gallardo-Garcia (Pl. 2, figs. G–H) seems to be similar to the materials collected by Nafarieh *et al.* (2019) from the Fars area (south Iran). The term conifer (cf) is used for this specimen due to incomplete skeletal structure and the absence of an equatorial section in our material.

The megalospheric test of *Assilina* cf. *laminosa* Gill (Pl. 2, fig. P) is discoidal to lenticular in shape and shows a medium to thick wall with an elongated periphery. It is smooth and characterized by laminations on the surface of the test as ornamentations. The central part of the test is covered by granules. The diameter of the test ranges from 7 mm to 10 mm and the thickness from 1.5 mm to 2 mm. This species is characterized by an internally laminated shell wall. This species is accompanied by *Assilina* cf. *granulosa* (d'Archiac), *Nummulites atacicus* Leymerie and *N. globulus* Leymerie. The stratigraphic range is attributed to the Early Eocene.

The megalospheric form of *Assilina* cf. *granulosa* (d'Archiac) (Pl. 2, fig. Q) is flattened to lenticular in shape and has a diameter of 5.5–7 mm and a thickness of 0.8–1 mm. This species shows thin to medium wall with a rounded periphery and a small depression in the central area. The granular ornamentations are well developed on the surface of the test. The spiral cord is thin to medium in thickness. This species is characterized by a heavily granulated surface with distinct septal ridges. It is associated with *Nummulites atacicus* Leymerie, *N. cf. fossulata* de Cizancourt, *N. globulus* Leymerie, and *Assilina* cf. *laminosa* Gill indicating the Ilerdian stage (SBZ 8).

The megalospheric test of *Assilina* cf. *khorrassanica* Rahaghi (Pl. 2, fig. R) is lenticular in shape and shows a thick wall with a sharp periphery and elevated central part. The central part of the test is covered by pustules. The diameter of the test ranges from 6 mm to 8 mm and the thickness from 2.5 mm to 3.5 mm. The present specimen is similar to Rahaghi's materials but differs by its smaller size. This species is distinguished from *A. cf. laminosa* Gill by its thicker wall and more elevated central part of the test. It is found in the Early Eocene limestone of the lower part of the North Gahrou section with the other assiliniids and nummulitids such as *Assilina* cf. *granulosa* (d'Archiac), *A. cf. laminosa* Gill, *Nummulites globulus* Leymerie and *N. atacicus* Leymerie.

Nummulites globulus Leymerie (Pl. 3, figs. I–J) is globular to biconical in shape with a diameter ranging from 2.5 mm to 2.9 mm and a thickness from 1 to 1–1.75 mm, for the A form. B-forms were not found in the examined samples. This species shows wedge-shaped chamber cavities with alar prolongations. The pillars are observed in the central part of the test. Septa are almost straight to slightly curved and angular towards the periphery. The chambers are uniformly rectangular to rhombic and increase gradually in size. There are 5 whorls in a radius of 1.375 mm in the equatorial section. The spacing of whorls increases slowly. The height of the chambers is larger than the width. The axial section is characterized by its biconvex form with the thick spiral lamina and the thick marginal cord. The *Nummulites globulus* Leymerie is distinguished from other associated *Nummulites* Lamarck by having a smaller and globular test, a rather smooth surface, thick spiral laminae, and almost straight to slightly curved

septa. The present specimen shows some similarities to those described by Blondeau (1972). The *Nummulites globulus* Leymerie is associated with *Nummulites atacicus* Leymerie, *Nummulites* cf. *fossulata* de Cizancourt, *Assilina* cf. *laminosa* Gill and *Assilina* cf. *granulosa* (d'Archiac) indicating the Ilerdian stage (SBZ 8). The biometrical data is documented in Figure 9.

Nummulites atacicus Leymerie (Pl. 3, figs. K–L) is lenticular in shape. The diameter of A-forms ranges from 3.3 to 3.5 mm and thickness from 1.7 mm to 2.7 mm. B-forms are not found in the examined samples. The equatorial section shows 5 whorls in a radius of 1.75 mm. The spacing of whorls increases slowly till the end. The septa are arched and inclined towards the periphery. The height of the chambers is larger than the width. The axial section is characterized by regular whorls, narrow spiral cavity, thick spiral lamina, and medium marginal cord. The pillars are observed in the central part of the test.

It is closely similar to *Nummulites praecursor* de la Harpe which is distinguished by the slightly larger size of the test with regular septa and more chambers per whorl (Racey, 1995). It is also often confused with *Nummulites globulus* Leymerie and *Nummulites discorbinus* Schlotheim from which it is distinguished by its small proloculus and more chambers per whorl.

The co-occurrences of *N. atacicus* Leymerie and *N. globulus* Leymerie represents an excellent global biostratigraphic marker of the Early Eocene (Middle Ilerdian). So, the stratigraphic range of this species is considered Ilerdian (SBZ 8). The biometrical data is documented in Figure 9.

Nummulites cf. *fossulata* de Cizancourt (Pl. 3, fig. C) is characterized by the small lenticular test with a central depression and sharp periphery. The shape of the test is an angular “dumb-bell” in an axial section. The biometric data are measured based on the axial section because, in the axial section, this species appears to be very unique. The test has a diameter of 1.75–1.85 mm and a thickness of 0.85–0.9 mm. This species is closely similar to the recorded specimens of Racey (1995). The *Nummulites* cf. *fossulata* de Cizancourt was originally found in Afghanistan by de Cizancourt (1938) in the Early Eocene. It was reported by Racey (1995) from Late Cuisian to Early Lutetian deposits. This species is reported for the first time from the Jahrum Formation in the study area. It is associated with *N. globulus* Leymerie and *N. atacicus* Leymerie, indicating an Early Eocene age.

The megalospheric form of *Nummulites* cf. *perforatus* (de Montfort) (Pl. 3, figs. G–H) shows an inflated test with a rounded periphery. The diameter of the test ranges between 4.5 mm and 7 mm and the thickness from 1.58 mm to 2.7 mm. The diameter of proloculus ranges from 0.6 to 0.85 mm. The spiral whorls are regular. No microspheric forms were found in our material. The septa are inclined and slightly curved. This species is associated with *Nummulites ptukhiani* Kacharava and *Assilina* cf. *granulosa* (d'Archiac) and its biostratigraphic range is assigned to Bartonian. Due to the absence of centered equatorial sections, we prefer to use the term conifer (cf.) to determine the taxa. The biometrical data is documented in Figure 9.

The megalospheric form of *Nummulites malatyensis* Sirel (Pl. 3, figs. D–F) shows an inflated lenticular test with a strongly rounded periphery. The diameter of the test ranges from 2.2 to 2.6 mm and the thickness from 1.6 mm to 1.75 mm. The spherical to sub-spherical proloculus has a diameter of

Species	A-form	D (mm)	T (mm)	W4th/R	(C) in 1/4 third whorl	H-L	Proloculus	Age
<i>Nummulites globulus</i> (after Blondeau, 1972)		2-3.5	1-1.8	4/1.3	5-6	H> L	————	Ilerdian (SBZ 8)
<i>N. globulus</i> (after Schaub, 1981)		2-3	1-1.5	4/1.2-1.7	————	H> L	0.15-1.3	Ilerdian (SBZ 8)
<i>N. globulus</i> (after Abdulsamad, 2000)		2.8	1.8	4/1.11	4-5	H> L	0.15-0.25	Ilerdian (SBZ 8)
<i>N. globulus</i> (in this study)		2.5-2.9	1-1.75	4/1.2	5-6	H> L	0.2-0.25	Ilerdian (SBZ 8)
<i>N. atacicus</i> (after Blondeau, 1972)		3-5	1.2-2.3	4/1.4	6-7	H> L	————	Ilerdian (SBZ 8)
<i>N. atacicus</i> (after Schaub, 1981)		3-5.5	1.3-2.5	4/1.8-2	————	H> L	0.4-0.65	Ilerdian (SBZ 8)
<i>N. atacicus</i> (in this study)		3.3-3.5	1.7-2.7	4/1.37	7	H> L	0.45-0.5	Ilerdian (SBZ 8)
<i>N. ptukhiani</i> (after Schaub, 1981)		2.8-4	1-1.8	————	————	————	0.15-0.22	Bartonian
<i>N. ptukhiani</i> (after Boukhari et al. 2005)		2.7-2.9	1.25-1.4	4/1.32	4-5	H=L	0.1-0.15	Priabonian
<i>N. ptukhiani</i> (after Cotton et al. 2019)		3.23	1.74	4/1.4	5-6	H> L H< L	————	Bartonian
<i>N. ptukhiani</i> (in this study)		3.2-4	1.5-1.9	4/1.38	5-6	H≈ L	0.25-0.35	Bartonian
<i>N. malatyensis</i> (after Sirel, 2003)		0.9-2.7	0.7-1.7	————	7-8	H=L	0.1-0.275	Bartonian
<i>N. malatyensis</i> (after Deveciler, 2013),		2.4-3.4	1.5-1.75	4/1.4	8-9	H> L	0.25-0.3	Bartonian
<i>N. malatyensis</i> (in this study)		2.2-2.6	1.6-1.75	4/0.9	————	H=L	0.25-0.35	Bartonian
<i>N. perforatus</i> (after Blondeau, 1972)		4-6	2-2.5- 3.2	6/2.1	5-6	H< L	————	Bartonian
<i>N. perforatus</i> (after Schaub, 1981)		3-5-6-7-9	1.5-2.5-3-4	5/2.5	————	H< L	0.75-1.25	Bartonian
<i>N. cf. perforatus</i> (in this study)		4.5-7	1.58-2.7	4/1.3-1.85	5-6	H< L	0.6-0.85	Bartonian

Fig. 9. Comparison of small A- forms based on biometrical data between *Nummulites* taxa of the study area and the specimens of Blondeau (1972), Schaub (1981), Abdulsamad (2000), Sirel (2003), and Deveciler (2013).

0.25–0.35 mm. The thickness of the spire is uniform in all whorls. The rate of the spiral opening increases gradually and is constant until the last whorl.

Nummulites malatyensis Sirel was first reported by Sirel (2003) in Bartonian limestone of the Develi section (Malatya). In this study area, this species was found in the calcareous rocks overlying the carbonate succession containing *Nummulites ptukhiani* Kacharava, *Alveolina* cf. *fusiformis*

Stache, *Gyroidinella magna* Le Calvez, and *Fabiania cassis* (Oppenheim). The biometrical data is documented in Figure 9.

Nummulites ptukhiani Kacharava (Pl. 3, figs. A–B) has a diameter of 3.2–4 mm and a thickness of 1.5–1.9 mm for 4 whorls, in the megalospheric form. The proloculus is 0.25–0.35 mm in diameter. No microspheric forms were found in our material. The spiral laminae are thick, up to half of the height of the chambers in

the inner whorls. Chambers are generally higher than wide in each spiral whorl. The pillars are visible and create granules at the surface of the test. The biometrical data is documented in Figure 9.

10 Discussion

The sedimentary model for Tethyan carbonate ramps was proposed by Buxton & Pedley (1989) based on sedimentological and biological characteristics common to depositional environments of present-day ramps (Purser, 1973; Reiss and Hottinger, 1984). Buxton and Pedley (1989) distinguished a succession of facies belts that extends from the protected zone of the inner ramp, characterized by peritidal and lagoonal muddy facies, to deeper zones of the middle and outer ramp.

The littoral zone (tidal flat) consists of rare foraminiferal facies, represented by mudstones and dolostone or dolomitic limestones. The mudstones contain thin shells of bivalves, scarce pellets, miliolids, and small rotaliids. This association represents an oligotypic community of epifaunal benthos and indicates a low-energy depositional setting (Zamagni *et al.*, 2008). The dolo-micritization is a diagenetic process in restricted sedimentary environments. The succession of dolostone and dolomitic limestone is usually formed in the low-energy domain of intertidal and subtidal environments in littoral to lagoonal settings (Wilson and Evans, 2002; Al-Saad, 2005; Ivanova *et al.*, 2008; Wilmsen *et al.*, 2010). The main sedimentological characteristic of these facies is a rhythmic alternation of mudstone and dolomitic limestone (dolostone). Therefore, the absence of planktic foraminifera and the presence of small porcellaneous foraminifera (miliolids) indicate low-energy environment with inshore condition in the littoral zone.

The lagoonal microfacies consist of miliolid-pellet wackestone facies, *Macetadiscus*-miliolid-pellet wackestone facies, and conical porcellaneous- agglutinated foraminifera-miliolid wackestone facies in Kuh-e- Soukhteh section, and *Macetadiscus*-miliolid-pellet wackestone facies, conical agglutinated foraminifera-*Alveolina*-pellet wackestone facies, and *Alveolina*- bioclastic- pellet wackestone facies in the North Gahrou section. These microfacies generally contain small porcellaneous foraminifera (miliolids), small rotaliids, large discoidal soritids, and agglutinated conical foraminifera. They spread in low-energy environments with relatively slow currents and hint to the restricted environment of the inner ramp (Geel, 2000; Rasser *et al.*, 2005; Badenas and Aurell, 2010). This interpretation is supported by the presence of carbonate mud and the absence of structures indicative of high-energy events.

The small porcellaneous foraminifera dominated the shallowest waters in the restricted lagoon in the inner ramp setting, while the large discoidal soritids (*Macetadiscus* Hottinger) and conical porcellaneous (*Neorhipidionina* Hottinger) foraminifera were restricted to the inner and proximal middle ramp. The high diversity of porcellaneous foraminifera was developed in meso- to oligotrophic shallow water environments (Reiss and Hottinger, 1984; Hallock, 1984, 1988; Buxton and Pedley, 1989; Romero *et al.*, 2002). The *Macetadiscus* bearing facies has a lateral paleoenvironmental relationship with the *Alveolina* facies. The presence of *Macetadiscus* Hottinger, Serra-Kiel and Gallardo-Garcia suggests relatively shallower water than the *Alveolina* facies. The *Alveolina* d'Orbigny is an important element in Lower and Middle Eocene shallow-water deposits. They are also

abundant in the lagoon or enclosure behind the back shoal as well as in the shoal and are found in relatively deeper water than *Orbitolites* Lamarck and *Macetadiscus* Hottinger, Serra-Kiel and Gallardo-Garcia. According to Hottinger (1983), the *Alveolina* facies can occur in protected shelf and higher energy shoal environments.

Porcellaneous foraminifera with large conical shapes occurred in tropical carbonate platforms within the upper part of the photic zone (Reiss and Hottinger, 1984; Hohenegger *et al.*, 2000). According to Nebelsick *et al.* (2005) and Barattolo *et al.* (2007), the Middle and Late Eocene larger conical porcellaneous foraminifera were restricted to the proximal middle ramp setting. The recorded facies (conical porcellaneous-agglutinated foraminifera-miliolid wackestone) represents shallow water setting with high light intensity and low substrate stability without turbidity. The conical agglutinated foraminifera are documented as the shallowest association of larger foraminifera, below tidal level, in the upper part of photic zone and indicate a depth of less than 40 m. The distribution of Paleogene conical agglutinated foraminifera depended to the nature of substrate. They seem to prefer the soft substrates and occur wackestone with fine-grained particles and mud. According to Vecchio and Hottinger (2007), the presence of mud level along with conical agglutinated foraminifera wackestone in the stratigraphic section, indicates low water energy environment that can occur in shallow water lagoon setting.

The shoal environment is represented by different facies types such as intraclast packstone and bioclastic grainstone in the Kuh-e- Soukhteh section and bioclast-intraclast packstone/grainstone, and *Gypsina*-lump-bioclast grainstone in the North Gahrou section. The shoal area is characterized by a great abundance of rounded bioclasts. The presence of skeletal grains, the high abundance of intraclasts, sparry calcite cement, and lack of lime mud in the shoal facies are also indicative of a high-energy environment.

The small and thin shelled hyaline foraminifera wackestone facies, and hyaline-porcellaneous foraminifera wackestone facies could be found in the back and fore shoals in the study area. These facies extend throughout the shallow water inner-middle ramp. The small and robust *Nummulites* Lamarck were spread throughout the Tethyan region from the eastern Alps to the Middle East (eastern Iran) and occurred in a broad range of open marine environments during the Eocene, whereas they are found within the inner ramp during the Paleocene (Rasser *et al.*, 1999; Romero *et al.*, 2002; Bassi *et al.*, 2007; Nebelsick *et al.*, 2005; Babazadeh, 2003). The co-occurrence of small *Nummulites* Lamarck and small thin shelled *Operculinas* d'Orbigny suggests shallow depth inner and middle ramp settings. It is affected by limiting conditions, such as slightly elevated nutrient levels, favoring the development of a community of r-selection strategists. Meanwhile, the small hyaline and agglutinated foraminifera (*Coskinolina* Stache) are shallow water dwellers and occurred in lagoon and open marine environments, at depth less than 40 m. (Ghose, 1977; Geel, 2000; Zamagni *et al.*, 2008). Therefore, the facies of small hyaline foraminifera wackestone can be distributed from the inner ramp to the proximal outer ramp (open marine) and shelves during the Early Paleogene.

The hyaline foraminifera such as *Rotalia* Lamarck, *Rotaliconus* Hottinger, and *Medocia* Parvati are not limited

to a specific environment and distributed from the inner ramp to proximal outer ramp (open marine), meanwhile the large hyaline foraminifera (*Assilina* d'Orbigny, *Nummulites* Lamarck, *Operculina* d'Orbigny, etc.) appeared in a broad range of open marine environments and occurred in deeper water (middle ramp to proximal outer ramp) and low energy setting during the Eocene. They were spread throughout the Tethyan realm from the eastern Alps to the Middle East (eastern Iran).

The hyaline-porcellaneous foraminifera wackestone facies is very heterogeneous due to the presence of two different types of foraminifera and is considered to occur in shallow water middle ramp setting. The small rotaliids and large soritids are representative of hyaline and porcellaneous foraminifera respectively. They are major contributors to Eocene carbonate sediments and present a wide geographic distribution. On the other hand, the co-occurrence of hyaline and porcellaneous foraminifera represents an open shelf platform or low relief with the connection between the front and behind relief. This suggests that no effective barrier existed (Romero *et al.*, 2002; Rasser *et al.*, 2005) and/or that porcellaneous foraminifera were transported from the shallow environment to deeper areas (Hohenegger *et al.*, 1999). A similar facies was reported from Paleogene carbonate ramp in western Cephalonia, Greece (Accordi *et al.*, 1998), Early Oligocene deposits of Lower Inn Valley (Nebelsick *et al.*, 2001), and Early Eocene deposits of Minerve section, France (Rasser *et al.*, 2005).

The fossil assemblage consisting of large foraminifera (k-strategist foraminifera, long life span) such as *Assilina* d'Orbigny and *Operculina* d'Orbigny with subordinate agglutinated foraminifera (*Valvulina* d'Orbigny), are thought to be restricted to stable, slightly nutrient-depleted environments, normal marine salinity values, and lower limit of the photic zone (Hallock and Glenn, 1986). Therefore, *Assilina* d'Orbigny and *Operculina* d'Orbigny in the large hyaline foraminifera wackestone/packstone facies were adapted to a reduced light condition in an open platform (ramp) and occurred in deeper water (proximal outer ramp) and low energy setting (Buxton and Pedley, 1989).

In the study section, all of the recorded shallow water benthic foraminiferal associations could be classified by the composition and morphology of the test in three groups: 1) porcellaneous, 2) agglutinated, and 3) hyaline. The Porcellaneous foraminiferal group is subdivided into three categories: a) simple forms, b) fusiform/discoidal forms, and c) planispiral/conical-fan forms.

The simple Porcellaneous foraminiferal forms have a small test with an imperforate wall. They consist of *Nuradanella* cf. *boluensis* Ozgen, *Biloculina* sp., *Triloculina* sp., and *Quinqueloculina* sp. *Alveolina fusiformis* Stache and *Alveolina elliptica* (Sowerby) are porcellaneous foraminifera with fusiform shape. While *Macetadiscus* cf. *incolumnatus* Hottinger, and *Orbitolites complanatus* Lamarck are porcellaneous foraminifera with discoidal shape. The planispiral-conical-fan shape forms consist of *Penarchaias glymijonesi* (Henson), *Archaias operculiniformis* Henson, *Rhabdorites malatyaensis* (Sirel), *Praerhapydionina delicate* Henson, *Haymanella huberi* (Henson), *Paraspirolina gigantea* Fleury, *Spirolina cylindracea* Lamarck, and *Neorhapydionina spiralis* Hottinger.

Four taxa including *Coskinolina perpera* Hottinger and Drobne, *Daviesiconus* cf. *balsilliei* (Davies), *Barattolites* sp.,

and *Valvulina* sp. are related to the agglutinated foraminiferal group.

The hyaline foraminiferal group is characterized by an association composed of nummulitids (*Nummulites* Lamarck, *Assilina* d'Orbigny and *Operculina* d'Orbigny) and rotaliids such as *Medocia blayensis* Parvati, *Rotaliconus persicus* Hottinger, *Gyroidinella magna* Le Calvez and *Fabiania cassis* (Oppenheim), *Asterigerina rotula* (Kaufmann), *Gypsina marianensis* Hanzawa, *Europertia* sp., and *Rotalia* sp.

The Early Eocene (Ypresian) age is indicated by the foraminiferal Assemblage A in the lower part of the North Gahrou section. Whereas typical late Middle Eocene (Bartonian) species related to Assemblages B and Assemblage C, are present in the upper part of North Gahrou and throughout Kuh-e-Soukhteh sections as well. The absence of Cuisian and Lutetian benthic foraminifera in the North Gahrou section is most probably due to a concealed fault unnoticed during fieldwork. At last, the stratigraphic studies improve the resolution of Eocene carbonate microfacies and benthic foraminiferal biozonation, which were poorly established in this region.

11 Conclusions

- In the study area, the Jahrum Formation consists of three main lithofacies: limestone, marl and dolostone/dolomitic limestone. It yields a rich benthic foraminiferal fauna that took place in the Tethyan carbonate ramp environment.
- Based on the stratigraphic range of index benthic foraminifera, three assemblage zones are recognized for the Jahrum Formation in the two studied sections: Assemblage A of the Gahrou section is assigned to the Early Eocene (Ypresian), while the Assemblage B of the Gahrou section and the Assemblage C of Kuh-e-Soukhteh section are considered late Middle Eocene (Bartonian) in age. These assemblages are comparable with the benthic foraminifera assemblages of west Tethys and neighboring countries in the Middle East and indicated an extension of the Neo-Tethys realm from the Zagros passive margin (west Iran) to the Sistan Suture Zone (east Iran).
- The absence of Cuisian and Lutetian benthic foraminifera between two assemblage zones in the North Gahrou section is related to fault disruption.
- The pattern of foraminiferal distribution in the Kuh-e-Soukhteh section shows a shallow water environment with relative deepening through time. Whereas, the distribution of microfacies in the North Gahrou section, indicates shallowing upward.
- The Jahrum Formation corresponds to the progressive onset of a carbonate ramp characterized by protected low-energy environments with scarce influence of tidal waves. The analysis of carbonate facies suggests a homoclinal ramp setting with the transition from inner ramp to proximal outer ramp on the gently seaward-sloping morphology.
- There was no evidence of re-sedimentation or turbidite sediments indicating breakage in the carbonate platform. Also, there are no reef-making fossil structures or large and important reefs that separate the open sea from the restricted and semi-restricted parts of the basin.

Acknowledgments. The authors greatly acknowledge the facilities provided by the Department of Geology of Payame Noor University. This research did not receive any specific grant from funding agencies in the public, commercial, or non-profit sectors. We thank the helpful and constructive reviews of the manuscript by Dr. C. Robin and an anonymous referee which enabled us to improve the manuscript. The authors are thankful for the editorial corrections, which were very helpful.

References

- Abdulsamad EO. 2000. Contribution to the Nummulites taxonomy from the Paleogene sequences of Al Jabal al Akhdar (Cyrenaica, NE Libya). *Revue de Paléobiologie* 19: 19–45.
- Accordi G, Carbone F, Pignatti J. 1998. Depositional history of a Paleogene carbonate ramp (Western Cephalonia, Ionian Islands, Greece). *Geologica Romana* 34: 131–205.
- Adams TD, Bourgeois F. 1967. Asmari biostratigraphy, geological and exploration division. Iranian Oil Offshore Company Report, 1074 (Unpublished).
- Agard P, Omrani J, Jolivet L, Mouthereau F. 2005. Convergence history across Zagros (Iran): constraints from collisional and earlier deformation. *International Journal of Earth Sciences (Geologische Rundschau)* 94: 401–19.
- Ahmad S, Jalal W, Ali F, Hanif M, Ullah Z, Khan S, et al. 2014. Using larger benthic foraminifera for the paleogeographic reconstruction of Neo-Tethys during Paleogene. *Arabian Journal Geoscience*: 1–18.
- Akhtar M, Butt A. 1999. Microfacies and foraminiferal assemblages from the Early Tertiary rocks of the Kala Chita Range (Northern Pakistan). *Géologie Méditerranéenne* 26: 185–201.
- Alavi M. 1994. Tectonics of the Zagros orogenic belt of Iran: new data and interpretations. *Tectonophysics* 229: 211–238.
- Alavi M. 2004. Regional stratigraphy of the Zagros fold-thrust belt of Iran and its proforeland evolution. *American Journal Sciences* 304: 1–20.
- Al-saad H. 2005. Lithostratigraphy of the Middle Eocene Dammam Formation in Qatar, Arabian Gulf: effect of sea-level fluctuations along a tidal environment. *Journal of Asian Earth Sciences* 25: 781–789.
- Babazadeh SA. 2003. Biostratigraphie et contrôles paléogéographiques de la zone de suture de l'Iran oriental. Implications sur la fermeture Téthysienne. Thèse de doctorat, France: Université d'Orléans, pp. 1–384.
- Babazadeh SA. 2008. Lower Eocene transgressive succession of Sahlabad province eastern Iran. Implication of biostratigraphy and microfacies analysis. *Revue de Paléobiologie* 27: 449–459.
- Babazadeh SA. 2010. Benthic foraminifera, microfacies analysis and paleoenvironmental interpretation of Early Eocene shallow water carbonate from Sahlabad province, eastern Iran. *Revue de Paléobiologie* 29: 305–317.
- Babazadeh SA. 2022. New agglutinated foraminifera from Early Eocene deposits of Mahallat region, Central Iran: Implication on biostratigraphy and paleoecology. *Revista Brasileira de Paleontologia* 25: 274–291.
- Babazadeh SA, Alavi M. 2013. Paleoenvironmental model for Early Eocene larger benthic foraminifera deposits from south Birjand region, East Iran. *Revue de Paléobiologie* 32: 223–233.
- Babazadeh SA, De Wever P. 2004a. Radiolarian Cretaceous age of Soulabest radiolarites in ophiolite suite of eastern Iran. *Bulletin de la Société Géologique de France* 175: 121–129.
- Babazadeh SA, De Wever P. 2004b. Early Cretaceous radiolarian assemblages from radiolarites in the Sistan suture (eastern Iran). *Geodiversitas* 26: 185–206.
- Babazadeh SA, Moghadasi SJ, Yoosefizadeh Baghestani N. 2015. Analysis of sedimentary basin based on the distribution of microfacies of Jahrum Formation in Dashte Zari, Shahrekord. In: *18th Geology Conference of Iran*. Tarbiat Modares University, pp. 649–655.
- Babazadeh SA, Pazooki Ranginlou S. 2015. Microfacies analysis and depositional environment of Jahrum Formation from Do kuhak region in Fars area, south Iran. *Disaster Advances Journal*: 21–28.
- Bachmann M, Hirisch F. 2006. Lower Cretaceous carbonate platform of the eastern Levant (Galilee and the Golan Heights): stratigraphy and second-order sea-level change. *Cretaceous Research* 27: 487–512.
- Badenas B, Aurell M. 2010. Facies models of a shallow-water carbonate ramp based on distribution of non-skeletal grains (Kimmeridgian, Spain). *Facies* 56: 89–110.
- Barattolo F, Bassi D, Romano R. 2007. Upper Eocene larger foraminiferal-coralline algal facies from the Klokova Mountain (southern continental Greece). *Facies* 53: 361–375.
- Bassi D, Hottinger H, Nebelsick JH. 2007. Larger foraminifera from the Upper Oligocene of the Venetian area, north-east Italy. *Palaeontology* 50: 845–868.
- Berberian M, King GCP. 1981. Towards a paleogeography and tectonic evolution of Iran. *Canadian Journal of Earth Sciences* 18 (2): 210–265.
- Beavington-Penney SJ, Racey A. 2004. Ecology of extant nummulitids and other larger benthic foraminifera, applications in paleoenvironmental analysis. *Earth Science Review* 67: 219–265.
- Beavington-Penney SJ, Wright VP, Racey A. 2006. The Middle Eocene Seeb Formation of Oman: An investigation of acyclicity, stratigraphic completeness, and accumulation rates in shallow marine Carbonate settings. *Journal of Sedimentary Research* 76: 1–25.
- Blondeau A. 1972. Les Numulites. De l'enseignement à la recherche des sciences de la terre. Paris: Vuibert, pp. 1–254.
- Boukhary M, Abdelghany O, Bahr S, Kamel YH. 2005. Upper Eocene larger foraminifera from the Dammam Formation in the border region of United Arab Emirates and Oman. *Micropaleontology* 51: 487–504.
- Burchette T, Wright VP. 1992. Carbonate ramp depositional systems. *Sedimentary Geology* 79: 3–57.
- Buxton MWN, Pedley HMA. 1989. Standardized model for Tethyan Tertiary carbonate ramps. *Journal of the Geological Society, London* 146: 746–748.
- Changaei K, Babazadeh SA, Arian M, Asgari Pirbaloti B. 2023. Systematic paleontology of Bartonian larger benthic Foraminifera from Shahrekord region in High Zagros, Iran. *Paleontological Research*, 27: 73–84.
- Cizancourt M. de 1938. Nummulites et Assilines du Flysch de Gardez et du Khost, Aghanistan Oriental. In: Cizancourt de M. de, Cox LR, eds. Contribution à l'étude des faunes Tertiaires de l'Afghanistan. *Mémoire de la Société Géologique de France* 39: 1–28.
- Cotton LJ, Pearson PN, Renema W. 2015. A new Eocene lineage of reticulate Nummulites (Foraminifera) from Kilwa district, Tanzania; a place for Nummulites ptukhiani? *Journal of Systematic Palaeontology*: 1–11.
- Deveciler A. 2010. The first appearance of the Bartonian benthic foraminifera at the Cayraz Section (north of Haymana, south Ankara, central Turkey). *Yerbilimleri* 31: 191–203.
- Deveciler A. 2013. Description of larger benthic foraminifera species from the Bartonian of Yakacık-Memlik region (N Ankara, Central Turkey). *Yerbilimleri* 35: 137–150.

- Dunham, R.J. 1962. Classification of carbonate rocks according to depositional texture. In: Ham WE, ed. Classification of carbonate rocks, pp. 108–121.
- Embry AF, Klovan JE. 1971. A Late Devonian reef tract on northeastern bank Island, Northwest Territories. *Bulletin of Canadian Petroleum Geology* 19: 730–781.
- Flügel E. 1982. Microfacies analysis of limestones. Berlin: Springer-Verlag, pp. 1–633.
- Flügel E. 2004. Microfacies of carbonate rock. Springer-Verlag, pp. 1–976.
- Geel T. 2000. Recognition of stratigraphic sequences in carbonate platform and slope deposits, empirical model based on microfacies analysis of Paleogene deposits in southeastern Spain. *Palaeogeography, Palaeoclimatology, Palaeoecology* 155: 211–238.
- Ghose BK. 1977. Paleoecology of the Cenozoic reefal foraminifera and algae—a brief review. *Palaeogeography, Palaeoclimatology, Palaeoecology* 22: 231–256.
- Hallock P. 1984. Distribution of selected species of living algal symbiont-bearing foraminifera on two Pacific coral reefs. *Journal of Foraminiferal Research* 9: 61–69.
- Hallock P, Glenn EC. 1986. Large foraminifera; a tool for paleoenvironmental analysis of Cenozoic carbonate depositional facies. *Palaios* 1: 55–64.
- Hallock P. 1988. Diversification in algal symbiont-bearing foraminifera: a response to oligotrophy? *Revue de Paleobiologie* 2: 789–797.
- Hohenegger J, Yordanova E, Hatta A. 2000. Remarks on west Pacific nummulitidae (foraminifera). *Journal of Foraminiferal Research* 30: 3–28.
- Hohenegger H, Yordanova E, Nakano Y, Tatzreiter F. 1999. Habitats of larger foraminifera on the upper reef slope of Sesoko Island, Okinawa, Japan. *Marine Micropaleontology* 36: 109–168.
- Hottinger L. 1983. Processes determining the distribution of larger foraminifera in space and time. *Utrecht Micropaleontological Bulletin* 30: 239–253.
- Hottinger L. 2007. Revision of the foraminiferal genus *Globoreticulina* Rahaghi, 1978, and of its associated fauna of larger foraminifera from the late Middle Eocene of Iran. *Carnets de Géologie/Notebooks on Geology*: 1–51.
- Hottinger L, Drobne K. 1980. Early Tertiary conical imperforate foraminifera. *Slovenska Akademija Znanosti in Umetnosti, Razprave* 22(3): 187–276.
- Ivanova D, Kof OB, Koleva R, Roniewicz E. 2008. Oxfordian to Valanginian paleoenvironmental evolution on the western Moesian carbonate platform: a case study from Sw Bulgaria. *Annales Societatis Geologorum Poloniae* 78: 65–90.
- James GA, Wynd JG. 1965. Stratigraphic Nomenclature of Iranian Oil Consortium Agreement Area. *American Association of Petroleum Geologists Bulletin* 49: 2182–2245.
- Kalantari A. 1976. Microbiostratigraphy of the Sarvestan Area, Southwestern Iran (Geological Laboratories Publication). Tehran: National Iranian Oil Company, pp. 1–129.
- Kalantari A. 1978. Paleocene Biostratigraphy of some part of Iran (Geological Laboratories Publication). Tehran: National Iranian Oil Company, pp. 1–165.
- Kalantari A. 1980. Tertiary Faunal Assemblage of Qum-Kashan, Sabzevar and Jahrom areas (Geological Laboratories Publication). Tehran: National Iranian Oil Company, pp. 1–126.
- Kalantari A. 1986. Microfacies of carbonate rocks of Iran, National Iranian Oil Company, Geological Laboratory Publication. Tehran: National Iranian Oil Company, pp. 1–520.
- Kalantari A. 1992. Lithostratigraphy, and microfacies of Zagros orogenic area S.W. Iran (Geological Laboratories Publication). Tehran: National Iranian Oil Company, pp. 1–421.
- Khatibi Mehr M, Moalemi A. 2009. Historical sedimentary correlation between Jahrom Formation and Ziarat Formation on the basis of benthic foraminifera. *Journal of Geology of Iran* 9: 87–102.
- Loeblich AR, Tappan H. 1987. Foraminiferal genera and their classification. New York: Van Nostrand Reinhold Co., pp. 1–970.
- Mirza K, Sameeni SJ, Munir M, Yasin A. 2005. Biostratigraphy of the Middle Eocene Kohat Formation, Shekhan Nala Kohat basin, Northern Pakistan. *Geological Bulletin of the Punjab University* 40–41: 57–66.
- Motiei H. 1993. Stratigraphy of Zagros, Treatise on the Geology of Iran. Iran Geological Survey of Iran, pp. 1–559.
- Motiei H. 1994. Geology of Iran: stratigraphy of Zagros. Tehran: Geological Survey of Iran Publication, pp. 1–583.
- Nafarieh E, Boix C, Cruz-Abad E, Ghasemi-Nejad E, Tahmasbi A, Caus E. 2019. Imperforate larger benthic foraminifera from shallow-water carbonate facies (Middle and Late Eocene), Zagros Mountains, Iran. *Journal of Foraminiferal Research* 49: 275–302.
- Nebelsick JH, Stingle V, Rasser M. 2001. Autochthonous facies and Allochthonous debris flows compared: Lower Oligocene carbonate of the Lower Inn valley (Tyrol, Austria). *Facies* 44: 31–46.
- Nebelsick JH, Rasser M, Bassi D. 2005. Facies dynamics in Eocene to Oligocene circumalpine carbonate. *Facies* 51: 197–216.
- Purser BH. 1973. The Persian Gulf, Holocene carbonate sedimentation and diagnosis in a shallow epicontinental sea. Berlin, Heidelberg, New York: Springer-Verlag.
- Racey A. 1995. Lithostratigraphy and larger foraminiferal (nummulitid) biostratigraphy of the Tertiary of northern Oman. *Micropaleontology* 41: 1–123.
- Rahaghi A. 1976. Contribution à l'étude de quelques grands foraminifères de l'Iran. *National Iranian Oil Company* 6: 1–84.
- Rahaghi A. 1978. Paleogene biostratigraphy of some part of Iran. *National Iranian Oil Company* 7: 1–165.
- Rahaghi A. 1980. Tertiary faunal assemblage of Qom-Kashan, Sabzevar and Jahrom area. *National Iranian Oil Company, Tehran* 8: 1–126.
- Rahaghi A. 1983. Stratigraphy and faunal assemblage of Paleocene and Lower Eocene in Iran. *National Iranian Oil Company* 10: 1–173.
- Racey A. 2001. Review of Eocene Nummulite accumulations: structure, formation and reservoir potential. *Journal of Petroleum Geology* 24: 79–100.
- Rasser MW, Less G, Baldi-Beke M. 1999. Biostratigraphy and facies of the Late Eocene of the Western Austrian Molasse Zone with special reference to the larger foraminifera. *Abhandlungen der Geologischen Bundesanstalt Wien* 56: 679–698.
- Rasser MW, Scheibner C, Mutti M. 2005. A paleoenvironmental standard section for Early Eocene tropical carbonate factories (Corberes, France; Pyrenees, Spain). *Facies* 51: 217–232.
- Reiss Z, Hottinger L. 1984. The Gulf of Aqaba. Ecological Micropaleontology. Springer-Verlag, pp. 1–354.
- Romero J, Caus E, Rosel J. 2002. A model for the paleoenvironmental distribution of larger foraminifera based on late middle Eocene deposits on the margin of the South Pyrenean basin. *Palaeogeography, Palaeoclimatology, Palaeoecology* 179: 43–56.
- Schaub H. 1981. Nummulites et Assilines de la Tethys Paleogène: taxinomie, phylogénèse et biostratigraphie. *Schweizerische paläontologische Abhandlungen* 104-106: 1–236.
- Serra-Kiel JS, Gallardo-Garcia A, Razin P, Robinet J, Roger J, Grelaud C, et al. 2016. Middle Eocene-Early Miocene larger foraminifera from Dhofar (Oman) and Socotra Island (Yemen). *Arabian Journal of Geosciences* 9: 1–95.
- Serra-Kiel JS, Hottinger L, Caus E, Drobne K, Ferrandez C, Jauhir AK, et al. 1998. Larger foraminiferal biostratigraphy of the

- Tethyan Palaeocene and Eocene. *Bulletin de la Société Géologique de France* 169: 281–299.
- Sirel E. 2003. Foraminiferal description and biostratigraphy of the Bartonian, Priabonian, and Oligocene shallow-water sediments of southern and eastern Turkey. *Revue de Paléobiologie* 22: 269–339.
- Sirel E. 2009. Reference sections and key localities of the Paleocene Stages and their very shallow/shallow-water three new benthic foraminifera in Turkey. *Revue de Paleobiologie* 28: 413–435.
- Smith LB. 2004. Full-controlled hydrothermal alteration of carbonate reservoirs: Geological association of Canada. Mineralogical Association of Canada Joint Annual Meeting St. Catherines, pp. 1–319.
- Stocklin J, Setudehnia A. 1991. Stratigraphic Lexicon of Iran (Report No.18). Tehran: Geological Survey of Iran, pp. 1–376.
- Takin M. 1972. Iranian Geology and continental drift in the Middle East. *Nature* 235: 147–50.
- Wilmsen M, Furisch FT, Seyed-Emami K, Majidifard MR, Zamani PM. 2010. Facies analysis of a large-scale Jurassic shelf-lagoon: the Kamar-e-Mehdi Formation of east-central Iran. *Facies* 56: 59–87.
- Wilson MEJ, Evans MEJ. 2002. Sedimentology and diagenesis of Tertiary carbonates on the Mangkalihat Peninsula, Borneo: implications for subsurface reservoir quality. *Marine and Petroleum Geology* 19: 873–900.
- Wynd JG. 1965. Biofacies of the Iranian oil consortium agreement area. Iranian Oil Operating Companies, Report 1082: 1–89.
- Zahedi M, Rahmati Ilkhechi M. 2006. Explanation of Geology of Shahrekord quadrangle, 1:250 000, pp. 1–194.
- Zamagni J, Mutti M, Kosir A. 2008. Evolution of shallow benthic communities during the Late Paleocene-Earliest Eocene transition in the Northern Tethys (SW Slovenia). *Facies* 54: 25–43.

Cite this article as: Babazadeh SA, Cluzel D. 2023. New biostratigraphy and microfacies analysis of Eocene Jahrum Formation (Shahrekord region, High Zagros, West Iran). A carbonate platform within the Neo-Tethys oceanic realm, *BSGF - Earth Sciences Bulletin* 194: 1.